PhD Course in Basic and Developmental Neuroscience

Head: Prof. Giovanni Cioni

Lack of Mid1, the mouse ortholog of the Opitz syndrome gene, causes abnormal development of the anterior cerebellar vermis

Tutor

Prof. Matteo Caleo

_____

Candidate

Alessio Lancioni

_____

CYCLE XXIII (2008-2010)
SSD: BIO/09

INDEX

1.Riassunto

La sindrome di G/BBB Opitz (OS) è un disordine genetico caratterizzato da difetti a carico della midline durante lo sviluppo. I pazienti maschi con la forma X-linked della sindrome di Opitz, causata da mutazione del gene MID1 con conseguente perdita di funzione, mostra un'alta variabilità nei sintomi clinici. MID1 codifica un'ubiquitina ligasi che controlla la fosfatasi 2A, ma il suo ruolo nella patogenesi di questa malattia è ancora poco chiaro. In questa tesi, descrivo una linea di topo in cui l'ortologo del gene umano MID1 non è funzionante. I topi knock out Mid1 mostrano un difetto anatomico del cervello presente anche nei pazienti, come l'ipoplasia della porzione anteriore del cervelletto e cioè del verme. Abbiamo osservato che la presenza di questo difetto è correlata con la coordinazione motoria e i deficit nell'apprendimento procedurale e non associativo. Il difetto è limitato alla parte anteriore dei lobi del cervelletto, e in particolare la regione durante lo sviluppo cerebellare adiacente al midbrain dorsale. Analisi durante la gestazione rivela che la mancanza di Mid1 causa l'accorciamento della parte posteriore del midbrain dorsale; la rostralizzazione del boundary midbrain/cervelletto; la down regolazione di Fgf 17 che è un fattore chiave nello sviluppo di questa regione. La mancanza di Mid1 causa una mis-specificazione del boundary tra midbrain/cerebellum che comporta quindi un anormale sviluppo della parte anteriore dei lobi del cervelletto. Questo animale modello rappresenta uno strumento per lo studio in vivo del ruolo fisiologico e patologico del gene Mid1 ed infine un sistema per analizzare lo sviluppo e la funzione del dominio anteriore cerebellare.

2. ABSTRACT

Opitz G/BBB Syndrome (OS) is a genetic disorder characterized by midline developmental defects. Male patients with the X-linked form of OS, caused by loss-of-function mutations in the MID1 gene, show high variability of the clinical signs. MID1 encodes an ubiquitin ligase that controls Phosphatase 2A but its role in the pathogenesis of the disease is still unclear. Here I report a mouse line carrying a non-functional ortholog of the human MID1 gene, Mid1. Mid1 null mice show the brain anatomical defect observed in patients, i.e. hypoplasia of the anterior portion of the medial cerebellum, the vermis. We found that the presence of this defect correlates with motor coordination, procedural and non-associative learning impairments. The defect is limited to the most anterior lobes of the vermis, the region of the developing cerebellum adjacent to the dorsal midbrain. Analyses at mid-gestation reveal that lack of Mid1 causes the shortening of the posterior dorsal midbrain; the rostralization of the midbrain/cerebellum boundary; and the down-regulation of a key player in the development of this region, Fgf17. Thus, lack of Mid1 causes a mis-specification of the midbrain/cerebellar boundary that results in an abnormal development of the most anterior cerebellar lobes. This animal model provides a tool for further *in vivo* studies of the physiological and pathological role of the Mid1 gene and a system to investigate the development and function of anterior cerebellar domains.

3. INTRODUCTION

2.1 Opitz G/BBB syndrome

Opitz G/BBB syndrome (OS) is a congenital anomaly disorder characterized by developmental defects of midline structures (Opitz, 1987). OS patients present hypertelorism, hypospadias and laryngo-tracheo-esophageal anomalies (Fig. 1). They may also have cleft of lip and palate, heart defects, and anal anomalies (Robin et al., 1996).

Opitz syndrome is genetically heterogeneous presenting with an autosomal dominant and an X-linked form (Robin et al 1995). The two forms cannot be differentiated on the basis of the clinical phenotype and in both the phenotype is more complex and more severe in male than in female patients (Robin et al 1996).

The autosomal dominant form is linked to a large region in 22q11.2 but the gene (or the genes) responsible has not yet been identified (Robin et al 1995).

Conversely, the gene implicated in the X-linked form of OS, MID1 (MIM# 300552), has been identified on the short arm of the X chromosome (Xp22.3) (Quaderi et al., 1997). In male OS patients, mutations have been found scattered throughout the entire length of the MID1 gene, suggesting a loss of function mechanism as the basis of this developmental phenotype.

In the X-linked OS form male patients manifest the clinical signs with variable expressivity whereas female carriers only show hypertelorism (Robin et al., 1995). A high percentage of X-linked OS patients present mental retardation and developmental delay and approximately one

third of the patients subjected to MRI show anatomical brain abnormalities that mainly consist of hypoplasia of the anterior cerebellar vermis (Fontanella et al., 2008).

Fig. 1 - Opitz Syndrome in two patients in the same family. Hypertelorism, laryngo-tracheo-esophageal anomalies and cleft of lip and palate are typically of this syndrome *(from Fontanella et al., Hum Mutat 29:584-59).*

2.2 Diagnosis/testing of Opitz Syndrome

The diagnosis of X-linked Opitz G/BBB syndrome is established most often by clinical findings. MID1 is the only gene currently known to be associated with X-linked Opitz G/BBB syndrome. Sequence analysis of the coding exons and intron-exon boundaries or mutation scanning using various techniques detects deletions, insertions, and missense, nonsense, and splice site mutations in 15%-45% of males with clinically diagnosed Opitz G/BBB syndrome. The cohorts tested for MID1 mutations often include simplex cases (i.e., individuals with no family history of Opitz G/BBB syndrome), who therefore cannot be determined to have either the X-linked form or the autosomal dominant form. The detection rate is higher in individuals with clear X-linked inheritance. The prevalence of X-linked Opitz G/BBB syndrome ranges from one in 50,000 to one in 100,000 males.

2.3 Management

Treatment of manifestations: management of anomalies by a multidisciplinary team; surgical treatment of medically significant laryngo-tracheo-esophageal malformations; tracheostomy as needed; standard surgical management of hypospadias, cleft lip/palate, imperforate anus, heart defects; speech therapy; neuropsychological and educational support. Prevention of secondary complications: antireflux measurements to minimize risk of aspiration. Surveillance: based on the type of malformations present; regular monitoring of hearing for those with cleft lip/palate.

2.4 Genetic counseling

X-linked Opitz G/BBB syndrome is inherited in an X-linked manner. In a family with more than one affected individual, the mother of an affected male is an obligate carrier. If the mother of a proband is a carrier, the chance of transmitting the disease-causing mutation in each pregnancy is 50%. Male offspring who inherit the mutation will be affected; female offspring who inherit the mutation will be carriers and will usually not be affected. Mildly affected males who have children will pass the disease-causing mutation to all of their daughters and none of their sons.

2.5 Clinical Diagnosis

The manifestations of X-linked Opitz G/BBB syndrome can be divided into major and minor findings based on frequency of occurrence. The findings show variable expressivity in affected individuals, even within the same family. The minimum requirements for the diagnosis of X-linked Opitz G/BBB syndrome are the presence of ocular hypertelorism at least one of the other

two major findings consistent with X-linked inheritance (Robin et al., 1996, De Falco et al., 2003).

Major findings

% Ocular hypertelorism and/or telecanthus (found in 100% of affected individuals)

% All degrees of hypospadias that, in the most severe form, can be associated with renal malformations (90%)

% Laryngo-tracheo-esophageal abnormalities, primarily laryngeal cleft, resulting in swallowing difficulties and respiratory dysfunction (70%)

Minor findings (found in <50% of individuals)

% Mental retardation and developmental delay

% Cleft lip and/or palate

% Congenital heart defects such as ventricular septal defect (VSD) or atrial septal defect (ASD), persistent left superior vena cava, patent ductus arteriosus

% Imperforate or ectopic anus

% Midline defects of the brain, such as agenesis of the corpus callosum and cerebellar vermis agenesis or hypoplasia observed by magnetic resonance imaging (MRI)

2.6 Genotype-Phenotype Correlations

Missense, nonsense, splice site, and frameshift mutations, insertions, and deletions all result in the same variable phenotype (Gaudenz et al., 1998, Cox et al 2000, De Falco et al., 2003, Winter et al., 2003, Pinson et al., 2004). The only exception is the observation of cerebellar anomalies in a high proportion (4/5) of individuals with R495X, the only recurrent MID1 mutation (Cox et al., 2000, De Falco et al., 2003, Pinson et al., 2004) and with the recently proposed correlation of a mild phenotype associated with mutations in the fibronectin type III domain of the protein (Mnayer et al., 2006). Opitz G/BBB syndrome was first reported as two separate entities, BBB syndrome (Opitz, Summitt et al., 1969) and G syndrome (Opitz, Frias et al., 1969). Subsequently, it has become apparent that the two syndromes identified in 1969 are in fact a single entity, now named Opitz G/BBB syndrome.

2.7 MID1

The gene responsible for the X-linked form of OS is MID1 (Quaderi et al., 1997). MID1 encodes an ubiquitin ligase that belongs to the Tripartite Motif (TRIM) family (Fig. 2). Indeed, MID1 is composed of a RING domain, two B-Box domains and a Coiled-Coil region (Tripartite Motif) and a subsequent FNIII and SPRY domains (Meroni and Diez-Roux, 2005). MID1 is associated with the microtubules (MT) and regulates the level of MT-associated Phosphatase 2A (PP2A) by binding alpha4 (Cainarca et al., 1999; Schweiger et al., 1999; Liu et al., 2001;

Trockenbacher et al., 2001). Recent data indicate that MID1 is involved in TNFα-induced p38MAPK-mediated apoptosis through the interaction with the alpha4/PP2A complex (Prickett and Brautigan, 2007). Mid1 expression during development was investigated in mouse, chicken and human. Mid1 is almost ubiquitously expressed at early embryonic stages becoming more restricted to the tissues involved in the disease during organogenesis (Dal Zotto et al., 1998; Richman et al., 2002; Pinson et al., 2004). In early chick development, Mid1 is also expressed on the right side ectoderm of the Hensen's node (Granata and Quaderi, 2003). Despite the biochemical and expression data, the role of MID1 in development and in the pathogenesis of OS is still obscure. The mutations found in OS patients indicate loss of function as the mechanism underlying the disease.

Fig.2 - MID1structure composed of a RING domain, two B-Box domains and a Coiled-Coil region (Tripartite Motif) and a subsequent FNIII and SPRY domains

2.8 The cerebellum

Although it represents only 10% of the total brain volume — hence the Latin name meaning 'little brain'— the mature cerebellum contains more than half of our neurons. It is therefore no

surprise that the cerebellum has a central role in our daily living. The cerebellum acts as a coordination centre, using sensory inputs from the periphery to fine-tune our movement and balance. Sensory information about movement and the position of body parts is sent to the so-called 'pre-cerebellar system', a group of nuclei in the brainstem. These nuclei, with the exception of the inferior olivary nucleus, in turn project to granule neurons, which communicate with the Purkinje cells of the cerebellum. The axons of the inferior olivary nucleus project directly to Purkinje cells. Granule neurons are glutamate- releasing, excitatory neurons, whereas Purkinje cells are inhibitory, using GABA (γ-aminobutyric acid) as their transmitter. There are three additional classes of cerebellar neuron: GOLGI cells, which contain GABA and glycine, and provide feedback inhibition to granule neurons, and the GABA-releasing STELLATE and BASKET cells, which modulate Purkinje cell output. The Purkinje neurons provide the primary output from the cerebellar cortex, projecting to the deep cerebellar nuclei. The neurons of the deep cerebellar nuclei finally project to the cerebral cortex, mediating the fine control of motor movements and balance. In addition to coordinating motion, the cerebellum has been implicated in motor learning and higher cognitive functions, but the circuitry involved in these activities is not yet understood.

Although the cerebellum is one of the first structures of the brain to differentiate, it achieves its mature configuration only many months after birth. This protracted development renders the cerebellum one of the more accessible brain structures to study.

2.9 Cerebellar development

The cerebellum develops from the dorsal region of the posterior neural tube. The embryonic cerebellum begins as little more than symmetric bulges into the early fourth ventricle: cerebellar hemispheres arise as mere buds from laminae on either side of the rhombencephalic midline, and the most rostral segment of the metencephalon produces outgrowths that form the first elements of the cerebellum. These lateral elements develop towards the midline and fuse in a rostral to caudal direction. As the primitive hemispheres come into contact with each other, they form first the superior and then the inferior vermis. The lateral elements from this fusion develop into the cerebellar hemispheres (Fig.3).

Cells in the cerebellum arise from two different germinal matrices. From the ventricular zone, cells radiate laterally and evolve into the deep cerebellar nuclei and Purkinje cells of the cerebellar cortex. The first cells to be born become the deep cerebellar nuclei at about week eight in human embryogenesis. At week nine, the ventricular zone begins to produce cells that will eventually form the Purkinje neurons. By 24 weeks, these proto-Purkinje cells send dendrites to the parallel fibers of the granule neurons. The full number of Purkinje cells is present early on, but their mature monolayer forms some time between 16 and 28 weeks postnatal.

Purkinje cells continue their maturation after birth, projecting to the deep cerebellar nuclei and refining the input they receive from the climbing fibers of inferior olivary neurons

From the ventricular zone, a third population of neurons is born after the formation of Purkinje cells. These neurons include the stellate, basket and Golgi interneurons that can be found in the molecular layer.

These three kinds of neurons have a modulatory action on the Purkinje cells and granule neurons.

Unlike most of the cell types of the cerebellum, which are born at the ventricular zone, cerebellar granule neurons come from a specialized germinal matrix called the rhombic lip. Migration of these primitive cells over the surface of the cerebellum starts as early as week 11 in humans; neuronal elements are present in the external granular layer (EGL) by week 27 (Fig. 4). Around birth, the granule neurons start they inward migration through the PC to find their final location in the internal granule layer (IGL). In the meanwhile, the smooth surface of the cerebellum starts the process of foliation, a series of remodelling steps that confer the final species/specific lobular architecture (Wang and Zoghbi, 2001; Chizhikov and Millen, 2003; Sillitoe and Joyner, 2007).

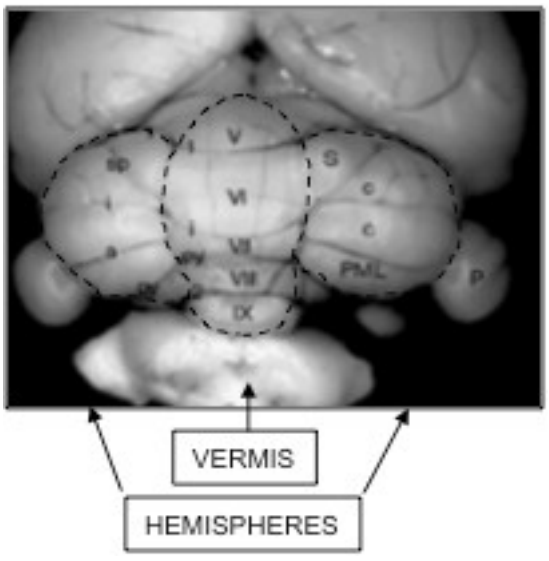

Fig. 3 - Cerebellum structure with central vermis and two lateral hemispheres with the typical lobular architecture.

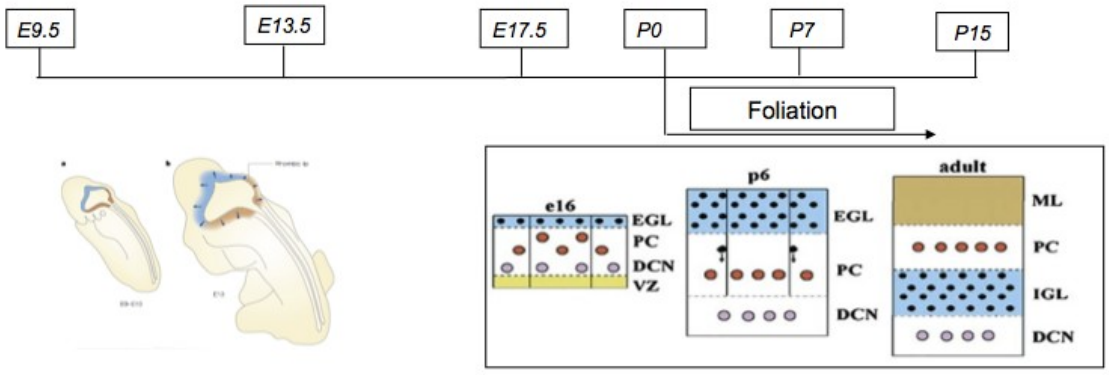

Fig. 4 - Schematic diagram of the developing cerebellum from E=9.5 to P15 demonstrating the extensive neuronal migrations that are required to achieve the final laminar structure of the adult cerebellum. In all diagrams ventricular zone (VZ) is yellow, Purkinje cell layer (PC) is white, external (EGL) and internal (IGL) granule cell layers are blue, and molecular layer (ML) is brown. Purkinje cells are red, granule cells are black and cells of deep cerebellar nuclei (DCN) are pink. The arrows show the directions of the cellular migration.

2.10 Genes in the developing cerebellar primordium

The neural tube can be thought of as comprising four different regions during early development. The most anterior portion of the neural tube, the prosencephalon, gives rise to the

forebrain. The mesencephalon, just caudal to the prosencephalon, gives rise to the midbrain, whereas hindbrain regions evolve from the metencephalon and myelencephalon.

The proper patterning of the mesencephalon and the metencephalon is dependent on molecular signals released from the ISTHMUS organizer (IO), which is located just caudal to the junction of these two regions. Morphologically, this region is marked by a sharp bend of the neural tube. It has been shown in various mouse mutants, as well as in transplant experiments, that the IO is necessary and sufficient for patterning the mid- hindbrain region from the neural tube. The IO is, in turn, set up by the expression of a complex array of genes. Two, in particular, are central to its development: Otx2, one of the mouse homologues of the Drosophila gene orthodenticle, and Gbx2, a homologue of the Drosophila gene unplugged. At embryonic day (E) 7.75, Otx2 is expressed in the mesencephalon, with a posterior boundary at the rostral metencephalon, whereas Gbx2 expression in the metencephalon is bounded anteriorly by the caudal mesencephalon (Ang et al., 1996; Wassaman et al., 1997). The sharp boundary between the expression domains of these two genes reflects their reciprocal repression (Broccoli et al., 1999; Millet et al., 1999). In addition to helping form the IO molecularly, Gbx2and Otx2 also regulate the expression of Fgf8 (fibroblast growth factor 8); Otx2 negatively regulates Fgf8 expression, whereas Gbx2 maintains it (Broccoli et al., 1999; Millet et al., 1999; Martinez et al., 1999). Fgf8 is involved in regulating the various genes expressed in the mid- and hindbrain regions. Mutant mice with a reduced level of Fgf8 expression have a severe patterning defect of the mid-/hindbrain region, which usually affects the cerebellum (Meyers et al., 1998). Fgf8 is a diffusible factor that exerts its action partially by inducing the expression of wingless-homologue 1 (Wnt1) through Lim homeobox 1b (Lmx1b) (Reifers et al., 1998; Adams et al.,

2000). Wnt1, in turn, maintains the expression of Engrailed (En1) (McMahon et al., 1992), which then positively regulates Fgf8 expression, completing the feedback regulatory loop.

Although the cross-regulation between Wnt1, En1 and Fgf8 is beginning to be understood, several other genes that are not part of this pathway are also important in patterning of the mid-/hindbrain region. The paired box genes Pax2 and Pax5 are expressed in the mid-/hind-brain region. Pax2-null mice never develop a cerebellum or posterior mesencephalon (Favor et al., 1996). Although Pax5 mutants have only a mild phenotype in the mid-/hind- brain region, mice with a Pax5 mutation against a Pax2 sensitized background lack a cerebellum and posterior midbrain (Urbanek et al., 1997). Pax2 and Pax5 might also be involved in the regulation of En1, Wnt1 and other patterning genes, and together constitute another positive regulatory loop (Broccoli et al., 1999).

The Hox gene family, which has an active role in patterning the hindbrain, seems to help to restrict the development of metencephalon structures into the myelencephalon. For example, Hoxa2 (homeobox A2), the most anteriorly expressed Hox gene, probably marks the caudal limit of the cerebellar anlage at rhombomere 1.

Bone morphogenetic proteins (Bmps) and sonic hedgehog (Shh) govern neuronal fates in the spinal cord; they have also been implicated in dorso-ventral patterning of the mid-/hindbrain region. Bmps can induce the cerebellar granule neuron marker mouseatonal homologue 1 (Math1) when expressed in the ventral neural tube of the region (Alder et al., 1999), and ectopic expression of SHH in the chick dorsal neural tube leads to ventralization of the neural tube and disruption of the mid-/hind- brain region (Zhang et al., 2000). Cerebellar development is also affected by ectopic expression of Shh, which leads to defects of the midline of the neural tube (Zhang et al., 2000). In sum, the reciprocal repression of Otx2 and Gbx2 forms the IO, which in

turn uses Fgf8 and En1 to pattern the prospective mid-/hindbrain region. Cells from both the mesencephalon and the metencephalon give rise to cerebellar tissues.

2.11 Cellular component

Purkinje cells - These cells are some of the largest neurons in the human brain, with an intricately elaborate dendritic arbor, characterized by a large number of dendritic spines. Purkinje cells are found within the Purkinje layer in the cerebellum. Purkinje cells are aligned like dominos stacked one in front of the other. Their large dendritic arbors form nearly two-dimensional layers through which parallel fibers from the deeper-layers pass. These parallel fibers make relatively weaker excitatory (glutamatergic) synapses to spines in the Purkinje cell dendrite, whereas climbing fibers originating from the inferior olivary nucleus in the medulla provide very powerful excitatory input to the proximal dendrites and cell soma. Parallel fibers pass orthogonally through the Purkinje neuron's dendritic arbor, with up to 200,000 parallel fibers forming a Granule-cell-Purkinje-cell synapse with a single Purkinje cell (Llinas et al., 2004). Each Purkinje cell receives a synapse from only a single climbing fiber. Both basket and stellate cells (found in the cerebellar molecular layer) provide inhibitory (GABAergic) input to the Purkinje cell, with basket cells synapsing on the Purkinje cell axon initial segment and stellate cells onto the dendrites.

Purkinje cells send inhibitory projections to the deep cerebellar nuclei, and constitute the sole output of all motor coordination in the cerebellar cortex.

Granule cells - Cerebellar granule cells, in contrast to Purkinje cells, are among the smallest neurons in the brain. They are also easily the most numerous neurons in the brain: In humans,

estimates of their total number average around 50 billion, which means that about 3/4 of the brain's neurons are cerebellar granule cells. Their cell bodies are packed into a thick layer at the bottom of the cerebellar cortex. A granule cell emits only four to five dendrites, each of which ends in an enlargement called a dendritic claw (Llinas et al., 2004). These enlargements are sites of excitatory input from mossy fibers and inhibitory input from Golgi cells.

The thin, unmyelinated axons of granule cells rise vertically to the upper (molecular) layer of the cortex, where they split in two, with each branch traveling horizontally to form a parallel fiber; the splitting of the vertical branch into two horizontal branches gives rise to a distinctive "T" shape. A parallel fiber runs for an average of 3 mm in each direction from the split, for a total length of about 6 mm (about 1/10 of the total width of the cortical layer). As they run along, the parallel fibers pass through the dendritic trees of Purkinje cells, contacting one of every 3–5 that they pass, making a total of 80–100 synaptic connections with Purkinje cell dendritic spines. Granule cells use glutamate as their neurotransmitter, and therefore exert excitatory effects on their targets.

Mossy fibers - Mossy fibers enter the granular layer from their points of origin, many arising from the pontine nuclei, others from the spinal cord, vestibular nuclei, etc. In the human cerebellum, the total number of mossy fibers has been estimated at about 200 million (Llinas et al., 2004). These fibers form excitatory synapses with the granule cells and the cells of the deep cerebellar nuclei. Within the granular layer, a mossy fiber generates a series of enlargements called rosettes. The contacts between mossy fibers and granule cell dendrites take place within structures called glomeruli. Each glomerulus has a mossy fiber rosette at its center, and up to 20 granule cell dendritic claws contacting it. Terminals from Golgi cells infiltrate the structure and make inhibitory synapses onto the granule cell dendrites. The entire assemblage is surrounded

by a sheath of glial cells. Each mossy fiber sends collateral branches to several cerebellar folia, generating a total of 20–30 rosettes; thus a single mossy fiber makes contact with an estimated 400–600 granule cells.

Climbing fibers - Purkinje cells also receive input from the inferior olivary nucleus (IO) on the contra lateral side of the brainstem, via climbing fibers. Although the IO lies in the medulla oblongata, and receives input from the spinal cord, brainstem, and cerebral cortex, its output goes entirely to the cerebellum. A climbing fiber gives off collaterals to the deep cerebellar nuclei before entering the cerebellar cortex, where it splits into about 10 terminal branches, each of which innervates a single Purkinje cell. In striking contrast to the 100,000-plus inputs from parallel fibers, each Purkinje cell receives input from exactly one climbing fiber; but this single fiber "climbs" the dendrites of the Purkinje cell, winding around them and making a total of up to 300 synapses as it goes (Llinas et al., 2004). The net input is so strong that a single action potential from a climbing fiber is capable of producing an extended complex spike in the Purkinje cell: a burst of several spikes in a row, with diminishing amplitude, followed by a pause during which activity is suppressed. The climbing fiber synapses cover the cell body and proximal dendrites; this zone is devoid of parallel fiber inputs.

Climbing fibers fire at low rates, but a single climbing fiber action potential induces a burst of several action potentials in a target Purkinje cell (a complex spike). The contrast between parallel fiber and climbing fiber inputs to Purkinje cells (over 100,000 of one type versus exactly one of the other type) is perhaps the most provocative feature of cerebellar anatomy, and has motivated much of the theorizing. In fact, the function of climbing fibers is the most controversial topic concerning the cerebellum. There are two schools of thought, one following

Marr and Albus in holding that climbing fiber input serves primarily as a teaching signal, the other holding that its function is to shape cerebellar output directly. Both views have been defended in great length in numerous publications. In the words of one review, "In trying to synthesize the various hypotheses on the function of the climbing fibers, one has the sense of looking at a drawing by Escher. Each point of view seems to account for a certain collection of findings, but when one attempts to put the different views together, a coherent picture of what the climbing fibers are doing does not appear. For the majority of researchers, the climbing fibers signal errors in motor performance, either in the usual manner of discharge frequency modulation or as a single announcement of an 'unexpected event'. For other investigators, the message lies in the degree of ensemble synchrony and rhythmicity among a population of climbing fibers.

Deep nuclei - Cross-section of human cerebellum, showing the dentate nucleus, as well as the pons and inferior olivary nucleus**.** The deep nuclei of the cerebellum are clusters of gray matter lying within the white matter at the core of the cerebellum. They are, with the minor exception of the nearby vestibular nuclei, the sole sources of output from the cerebellum. These nuclei receive collateral projections from mossy fibers and climbing fibers, as well as inhibitory input from the Purkinje cells of the cerebellar cortex. The three nuclei (dentate, interpositus, and fastigial) each communicate with different parts of the brain and cerebellar cortex. The fastigial and interpositus nuclei belong to the spinocerebellum. The dentate nucleus, which in mammals is much larger than the others, is formed as a thin, convoluted layer of gray matter, and communicates exclusively with the lateral parts of the cerebellar cortex. The flocculonodular lobe is the only part of the cerebellar cortex that does not project to the deep nuclei — its output goes to the vestibular nuclei instead (Llinas et al., 2004).

The majority of neurons in the deep nuclei has large cell bodies and spherical dendritic trees with a radius of about 400 μm, and use glutamate as their neurotransmitter. These cells project to a variety of targets outside the cerebellum. Intermixed with them is a lesser number of small cells, which use GABA as neurotransmitter and project exclusively to the inferior olivary nucleus, the source of climbing fibers. Thus, the nucleo-olivary projection provides an inhibitory feedback to match the excitatory projection of climbing fibers to the nuclei. There is evidence that each small cluster of nuclear cells projects to the same cluster of olivary cells that send climbing fibers to it; there is strong and matching topography in both directions.

When a Purkinje cell axon enters one of the deep nuclei, it branches to make contact with both large and small nuclear cells, but the total number of cells contacted is only about 35 (in cats).

2.12 History

The distinctive appearance of the cerebellum caused even the earliest anatomists to recognize it. Aristotle and Galen, however, did not consider it truly part of the brain: They called it the parencephalon ("same-as-brain"), as opposed to the encephalon or brain proper. Galen was the first to give an extensive description, noting that the cerebellar tissue seemed more solid than the rest of the brain he speculated that its function is to strengthen the motor nerves.

Further significant developments did not come until the Renaissance. Vesalius discussed the cerebellum briefly, and the anatomy was described more thoroughly by Thomas Willis in 1664. More anatomical work was done during the 18th century, but it was not until early in the 19th century that the first insights into the function of the cerebellum were obtained. Luigi Rolando in 1809 established the key insight that damage to the cerebellum results in motor disturbances. Jean Pierre Flourens in the first half of the 19th century carried out detailed experimental work, which revealed that animals with cerebellar damage can still move, but with a loss of coordination (strange movements, awkward gait, and muscular weakness), and that recovery after the lesion can be nearly complete unless the lesion is very extensive. By the dawn of the 20th century, it was widely accepted that the primary function of the cerebellum relates to motor control; the first half of the 20th century produced several detailed descriptions of the clinical symptoms associated with cerebellar disease in humans.

4. MATERIALS AND METHODS

3.1 Animals

All mouse were housed and handled in accordance with guidelines of the Institutional Animal Care and Use Committee, Cardarelli Hospital, Naples, Italy. $Mid1^{-/+}$ heterozygous females were generated by mating the male chimeras obtained upon injection of a $Mid1^{-/Y}$ ES clone with C57BL/6 females. $Mid1^{-/Y}$ mice and their $Mid1^{+/Y}$ control littermates were generated by mating heterozygous female with wild-type males. Mice were bred for 10 generations with C57BL/6 mice to generate and analyze the mutant mice in a pure genetic background.

3.2 Tissue preparation

Mice were anesthetized and perfused transcardially with 4% paraformaldehyde. Adult and postnatal brains were harvested and processed using standard procedures either for embedding in OCT and cryosectioning (20 μm) or agarose embedding and vibratome sectioning (50 μm). For time-pregnant mice, the day of the vaginal plug was designated E0.5. Embryos were collected, fixed in 4% paraformaldehyde, embedded in OCT and cryosectioned (20 μm).

3.3 RNA in situ hybridization (ISH)

Digoxigenin-labeled anti-sense riboprobes were generated for Pax2, Otx2, En1 (V. Broccoli, DiBIT Milan, Italy), Fgf17 (D. Ornitz, Washington University School of Medicine, St. Louis, Missouri) and ISH performed on cryosections (Surace et al., 2000). The sections were treated in RIPA buffer (Igepal 1%, NaCl 150mM, Na deoxycholate 0.5%, SDS 0.1%, EDTA 1mM and

Tris PH=8.0 50mM) and after fixed in 4% paraformaldeyde at room temperature for 15 min. The sections were washed in Pbs 1X and treated with Triethenolammine and Acetic Acid for 15 min, and Prehybridized for 1 hour at room temperature with 300 µl of Hybridation buffer (Formammide 50%, SSC 5X, Denhardts 5X, Herring sperm DNA 500 µg/ml and Yeast RNA 250 µg/ml) for each slides. The Hybridation with the probe was performed O.N. in a humidified chamber at 70 C. The second day the sections were washed in MABT (Maleic Acid 100mM pH=7.5, NaCl 150mM and Tween-20 0.1%) and blocked in a buffer composed by MABT and 10% sheep serum for 1 hour at room temperature. The slides were incubated with anti-DIG antibody diluited 1: 2000 O.N. at 4 C. The third day the sections were washed in a buffer (Tris PH=9.5 100mM, MgCl2 50ml, NaCl 100mM and Tween-20 0.1%) for 30 min. at room temperature and developed in the dark with NBT – BCIP Sigma.

3.4 Immunohistochemistry and Histology

Immunohistochemistry was performed using standard protocols.

Anti-Calbindin antibody: sections were washed in Phosphatebufferedsaline (PBS 1X) buffer (10Mm Tris-HCl, 200mM NaCl, 0.05% NP 40, 0.05% TWEEN 20) and treated in ethanol and hydrogen peroxide. The cryosections were blocked with a blocking solution composed of PBS1X and 20% NBS (Normal Bovine Serum) for 30min at room temperature and incubated with anti-Calbindin (Swant, Bellinzona, Switzerland; 1:20,000 on postnatal vibratome sections; 1:2,000 on embryo cryosections) over night at 4 C. The second day the antibody was detected detected using anti-rabbit biotinylated secondary antibody (1:200) and the ABC kit (Vector Laboratories).

Anti-Ki67 antibody: Cryosections were washed in Phosphatebufferedsaline (PBS 1X) buffer (Tris-HCl 10mM, NaCl 200mM, NP 40 0.05%, TWEEN 20 0.05%) then treated in citric buffer. After a brief wash in PBS 1X the sections were blocked in a standard blocking solution for 1 hour at room temperature and incubated with anti-Ki67 (DakoCytomation monoclonal rat anti-mouse, Clone TEC-3 cod. M7249) over night at 4 C.

The second day, the slides were treated with PBS 1X and hydrogen peroxide and detected using anti-rat biotinylated secondary antibody (1: 200) and the ABC kit (Vector Laboratories).

Anti-phopspho Histone H3: Crosections were washed in Phosphatebufferedsaline (PBS 1X) buffer (Tris-HCl 10mM, NaCl 200mM, NP 40 0.05%, TWEEN 20 0.05%) and blocked (blocking solution composed of Phosphate buffer 0.1M, DMSO 1%, Calf Serum 5%, Triton 0.05%) for 1h at room temperature. The sections were incubated over night at 4C with Anti-phospho Histone H3 (1: 100). The second day the antibody was detected detected using anti-rabbit biotinylated secondary antibody (1:200) and the ABC kit (Vector Laboratories).

3.5 Nissl Staining

Brain sections were fixed in 4% paraformaldehyde, then washed in Phosphatebufferedsaline (PBS 1X) buffer (10Mm Tris-HCl, 200mM NaCl, 0.05% NP 40, 0.05% TWEEN 20) and stained with Nissl Solution for 7 min at room temperature. Cryosections were dried in ethanol, fixed in xylene, and mounted with the EUKITT mounting kit (O. Kindler GmbH & CO).

3.6 Hematoxilin and Eosin Staining (H&E)

Embryos and various tissues were collected at different age. Samples were cryosectioned at 10- to 20- μm thickness.

Cryosections of tissues were fixed in 4% PFA, then washed in Phosphatebufferedsaline (PBS 1X) buffer (10Mm Tris-HCl, 200mM NaCl, 0.05% NP 40, 0.05% TWEEN 20) and stained in haematoxylin for 4 minutes and in eosin for 6 minutes. Cryosections were dried in ethanol, fixed in xylene, and mounted with the EUKITT mounting kit (O. Kindler GmbH & CO).

3.7 Masson's Trichrome Staining

Cryosections of various tissues were fixed in Bouin's Solution at 56° C for 15 min, cooled and washed in running tap water to remove the yellow color from the section. They were stained in Working Weigert's Iron Haematoxylin Solution for 5 min, washed in running tap water for 5 min and stained in Biebrich Scarlet- Acid Fucsin for 5 minutes, then rinsed in deionised water, placed in Working Phosphotungstic\Phosphomolybdic acid solution for 5 minutes, stained in Aniline Blue solution for 5 minutes and in acid acetic 1% for 2 minutes.

3.8 Statistical analysis

One-way ANOVA with a between group factor genetic (2 levels: wild-type, $Mid1^{-/Y}$) was used to analyze the data of the walking wire and the hanging wire tasks. Two-way ANOVA for repeated measures with a between group factor genetic (2 levels: wild-type, $Mid1^{-/Y}$) and testing days or training trials as repeated measures for horizontal activity (6 levels: T1-T6), latency to fall off the rod (5 levels: D1-D5), percentage of startle amplitude (3 levels: D1-D3), and percentage of correct response in the cross maze tasks (5 levels: D1-D5). Duncan post hoc test was used when appropriate. Statistical significance was set at $p< 0.05$. IC length was determined using photos of sagittal sections in ImageJ and evaluated by Student's t-test analysis.

5. RESULTS

4.1 Mid1$^{-/Y}$ mice show cerebellar defects

To study Mid1 function in *vivo*, in the laboratory a mouse line carrying a non-functional Mid1 gene by disruption of the first ATG-containing exon was generated. The replacement targeting vector used contained 6 kb of 5' and 4.5 kb of 3' homologous genomic sequences flanking the neoR cassette to allow homologous recombination, and a DTA cassette for negative selection of ES cells (Fig. 5a).

Southern blot analysis of DNA from a wild-type and the correct Mid1 recombinant ES clone was performed and showed the band of the expected reduced the size in Mid1 gene male mutant mice (Fig. 5b).

The correct recombinant clone was injected into C57BL/6 blastocysts. The resulting male chimeras were then mated to C57BL/6 females to obtain Mid1$^{-/+}$ heterozygous females upon germline transmission. The C57BL/6 mice have been used for next generations to obtain animals in pure C57BL/6 background.

Northern blot analysis on total RNA extracted from E11.5 Mid1$^{+/Y}$ and Mid1$^{-/Y}$ embryos using a Mid1 probe spanning exon 1-5 was performed and Mid1 expression was observed only in wild-type animals. Expression of the Gapdh gene was used as control (Fig. 5c).

RT-PCR analysis of RNA from tissues (heart, kidney, and liver) of $Mid1^{+/Y}$ and $Mid1^{-/Y}$ adult mice show the complete absence of the Mid1 transcript in male mutant mice (Fig. 5d) In this case the expression of the nucleolin gene was used as control.

Consistently, immunoblot analysis with a specific antibody shows the complete absence of the Mid1 protein in $Mid1^{-/Y}$ lysates. Immunoblot analysis of adult brain lysates (50 µg) using a Mid1 antibody (abcam ab70770) shows that the 70-75 kDa expected band is observed only in wild-type mice and is absent in two different $Mid1^{-/Y}$ mice (Fig. 5e).

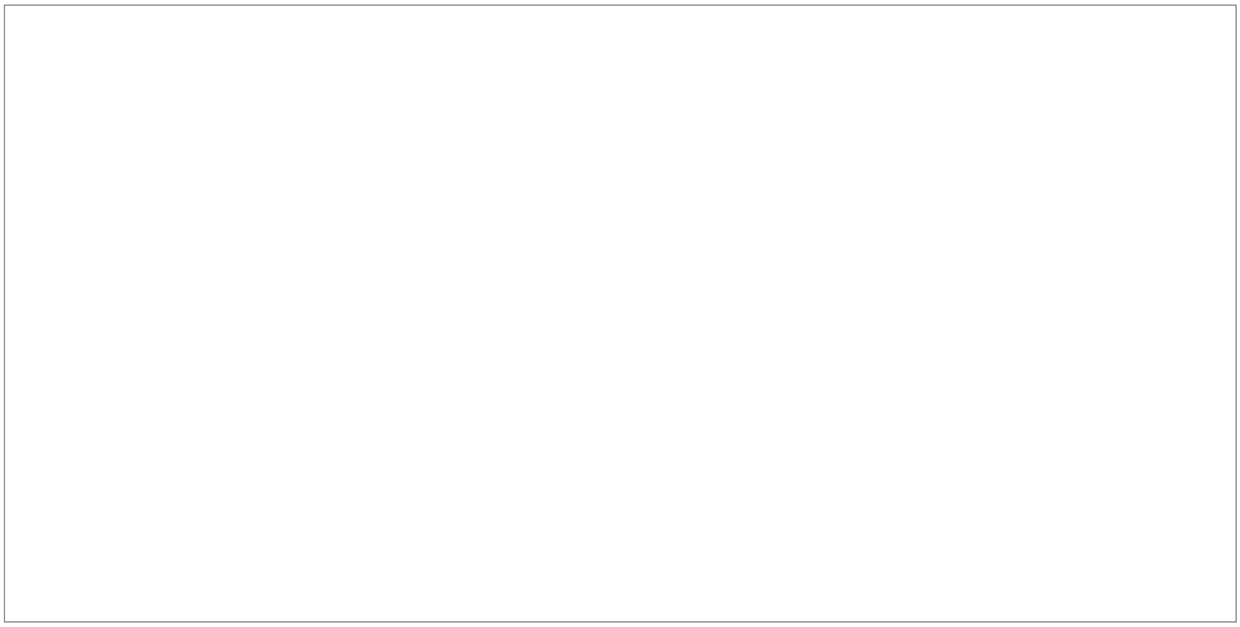

Fig. 5 - Generation of a $Mid1^{-/Y}$ mouse line by targeted recombination. A) Schematic representation of the replacement strategy with the wild-type Mid1 locus, the targeting vector, and the resulting non-functional Mid1 allele by disruption of the first ATG containing exon. The gene targeting vector was constructed by replacing a fragment containing the first coding exon of mouse Mid1 with the selectable neomycin resistance gene flanked by two lox sites. B) Southern blot analysis of DNA from a wild-type and the correct Mid1 recombinant ES clone. Sizes of the wild-type and the targeted allele are indicated. C) Northern blot analysis on total RNA extracted from E11.5 $Mid1^{+/Y}$ and $Mid1^{-/Y}$ embryos Mid1 expression is observed only in wild-type animals. Expression of the Gapdh gene is shown as control. D) RT-PCR analysis of RNA form tissues (heart, kidney, and liver) of $Mid1^{+/Y}$ and $Mid1^{-/Y}$ adult mice. Mid1 expression is observed only in wild-type animals. Expression of the nucleolin gene is shown as control. E) Immunoblot analysis of adult brain lysates (50 µg) using a Mid1 antibody (abcam ab70770) shows

that the 70-75 kDa expected band is observed only in wild-type mice and is absent in two different $Mid1^{-/Y}$ mice. SNAP25 antibody was used as protein loading control.

Like in human, Mid1 is transcribed from the X chromosome, although in mouse it spans the pseudoautosomal boundary (Palmer et al., 1997).

$Mid1^{-/Y}$ males and $Mid1^{-/-}$ females were indistinguishable from their wild-type and heterozygous littermates. We focused on male $Mid1^{-/Y}$ as null mutants using $Mid1^{+/Y}$ littermates as wild-type controls.

Direct observation of whole mount adult brains suggested a somewhat abnormal midbrain/cerebellum junction region in $Mid1^{-/Y}$ mice. Histological analyses confirmed the presence of a malformed anterior cerebellum. Nissl staining of sagittal sections through the vermis showed hypoplasia and abnormalities of lobes I, II, and III. The defect is present, although with a certain degree of variability, in all the $Mid1^{-/Y}$ mice analyzed (n=9) and in none of their wild-type littermates (n=7). In all null mice, lobe I, which is poorly pronounced in the C57/B6 mouse strain, is totally missing and lobe II is not completely formed. In many cases, the

third lobe is also abnormal in shape (Fig. 6a-b). Sagittal sections through the lateral hemispheres showed normal foliation (Fig. 6c-d)

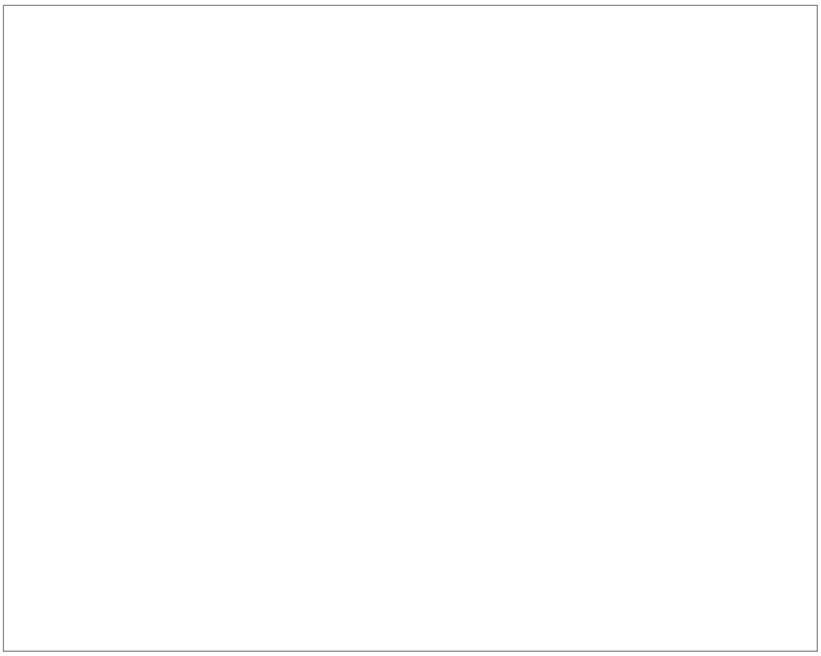

Fig.6 - Abnormal cerebellum in Mid1$^{-/Y}$ mice. Sagittal sections through the cerebellar vermis (A, B) and hemisphere (C, D) of adult wild-type and null mice stained with Nissl. Anterior is to the left. The numbers of the vermal and names of lateral lobes are indicated. The arrow in B indicates the anterobasal defect in Mid1$^{-/Y}$ mice.

To investigate the layer organization of the Mid1$^{-/Y}$ adult cerebellar cortex, we analyzed the two main neuronal populations of the cerebellum, Purkinje cells (PCs) and granule neurons. The Mid1$^{-/Y}$ general cerebellar cortex layer architecture is normal, with PCs disposed in monolayer and their dendritic arbors directed towards the external surface to define the molecular layer (ML) and with the internal granule cell layer (IGL) positioned just inside the PC monolayer.

Although abnormal in shape, even the anterior vermal lobes maintain the correct layer organization and thickness (Fig. 7a-d). The shape of the anterior lobes varies among mutant animals and, as shown in the coronal section through the anterior part of the cerebellum, the defect is not uniform along the medio-lateral axis where the presence of intermingled lobes and layers is observed (Fig. 7e-h). The coronal sections confirm the normal structure of lobe IV and of the hemispheres (Fig. 7-e-h)

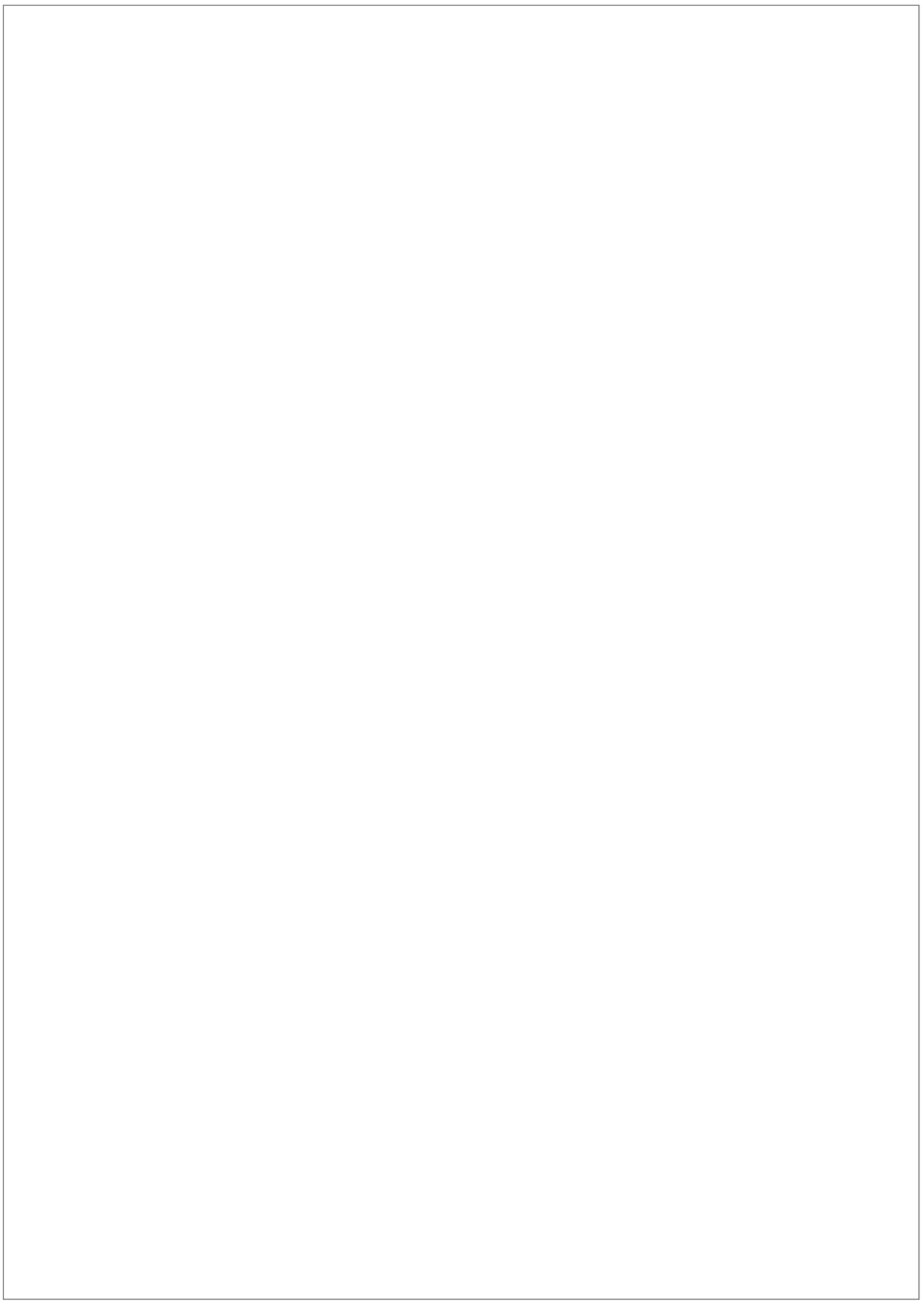

Fig.7 - Normal molecular layer (ML) and internal granule layer (IGL) organization in Mid1$^{-/Y}$ adult mice. Sagittal sections through the vermis (A-D) and coronal sections at the level of the anterior cerebellum (E-H). The insets show magnification of the indicated areas. In null mice, PCs and their dendrites form a normal ML (detected by anti- Calbindin) and granule cells form a normal IGL (detected by anti-NeuN). Numbers of the vermal lobes are indicated in E; h, hemisphere. The arrows indicate the defect in Mid1$^{-/Y}$ brains.

4.2 Cerebellar defects in Mid1$^{-/Y}$ originate prenatally

The development of the cerebellum is a long process that in the mouse begins as early as E9.5 and is completed by the second postnatal week (Chizhikov and Millen, 2003). Foliation begins around birth and reaches the definitive strain-specific architecture by postnatal day 15 (P15) (Sillitoe and Joyner, 2007). We analyzed sagittal sections of cerebella at P0, P2, and P7 (Fig. 8).

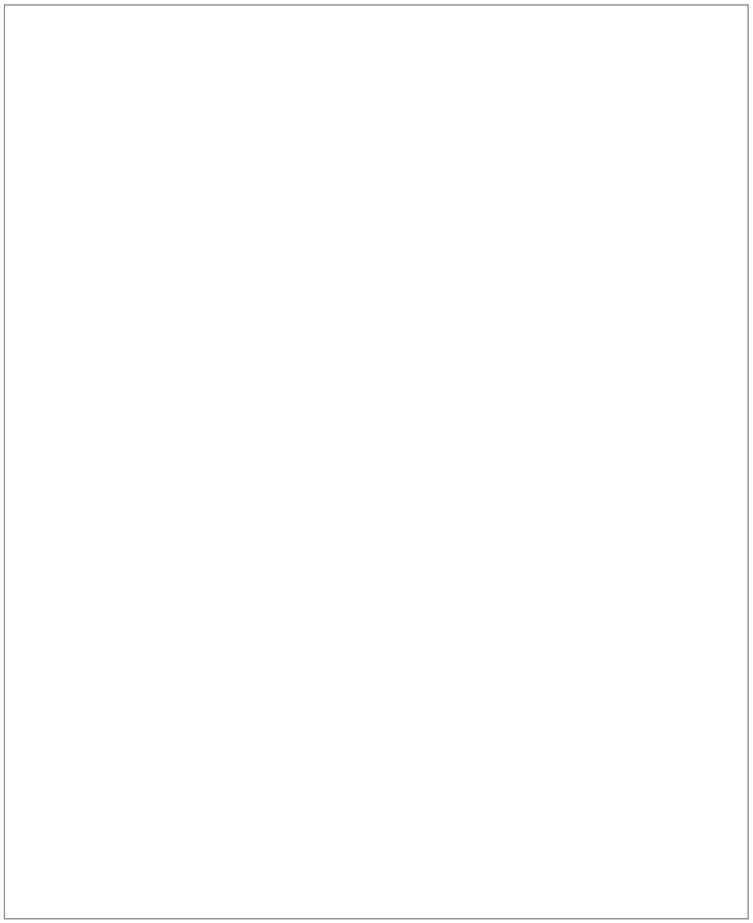

Fig. 8- .The anterobasal lobe defect in Mid1$^{-/Y}$ mice is detected at birth. Sagittal sections through the vermis at birth (A, B), P2 (C, D), and P7 (E, F) stained with Nissl. The granule cells at P0 and P2 are still superficial and form the EGL while at P7 they are starting to migrate inwards to eventually form the IGL. The 4 principal fissures (pc, preculminate; pr, primary; sec, secondary; pl, posterolateral) are normally formed in P0 and P2 Mid1$^{-/Y}$ mice. The cardinal lobes generated by the principal fissures are

correctly formed with the exception of the anterobasal lobe, rostral to the preculminate fissure, that shows the defect (ab, anterobasal; ad, anterodorsal; c, central; p, posterior; I, inferior). The development of the other cardinal lobes into the definitive foliation proceeds normally from P0 through P7. The asterisks indicate the principal fissures. The arrows indicate the defect.

At P0 and P2 the correct formation of the 4 principal fissures was observed in both wild-type and null mice (Fig. 8a-d). The principal fissures determine the anchor points for the formation of the 5 cardinal lobes. The anterobasal cardinal lobe, which gives rise to the definitive lobes I, II, and III, is limited caudally by the preculminate fissure and rostrally by the isthmus; it appeared abnormal already in P0 and P2 Mid1$^{-/Y}$ cerebella as shown by the upturning external granule layer (EGL) in the most anterior part and by a more profound fissure delimiting future lobes II and III (Fig. 8a-d). Consistent with the normal layer organization observed in adult mice, the granule cells at P0 form the EGL and progressively start their inward migration in both genotypes at P2 and P7 (Fig. 8c-f).

Thus, Mid1$^{-/Y}$ mice present developmental defects resulting in the postnatal abnormal formation of the anterobasal cerebellar vermis.

4.3 Mid1$^{-/Y}$ vermal defect is caused by an incorrect definition of the tectum-cerebellum boundary

The defect is present as early as the formation of the primitive fissures around birth, we therefore analyzed the developing vermis prior to that stage. At embryonic day 17.5 (E17.5) the surface of the cerebellum is smooth and the mutant is almost indistinguishable from the wild-type. Disordered PCs are still disposed in multilayers underneath the EGL in both genotypes (Fig. 9). However, in the most anterior Mid1$^{-/Y}$ cerebellum some PCs are present in ectopic position within the isthmic region heading towards the tectum (Fig. 9a-b).

Fig.9 - Inaccurate definition of the dorsal midbrain/cerebellum boundary in Mid1$^{-/Y}$ mice. Immunohistochemistry with anti-Calbindin (A, B) and RNA in situ hybridization (En1) followed by anti-Calbindin (C-D') on medial sagittal sections of E17.5 brains. C' and D', magnification of the delimited areas. IC, inferior colliculus; Cb, cerebellum; Is, isthmus; the arrows indicate ectopic PCs in Mid1$^{-/Y}$ embryos.

Analysis of the expression of Engrailed 1 (En1), a gene expressed in the tectum and the cerebellum, showed that PCs migration in ectopic position coincides with a premature halt of the anterior EGL. The strong En1 expression in the inferior colliculus (IC) also highlights a more rostral IC/ cerebellar boundary and a slightly enlarged isthmic region in Mid1$^{-/Y}$ embryos (Fig. 9c-d). These results suggest that the abnormal foliation presented by Mid1$^{-/Y}$ mice might not be the result of a fissure formation anomaly, rather, the consequence of a poor definition of the boundary between the posterior tectum, i. e. the inferior colliculus, and the most anterior part of the medial cerebellum. At mid-gestation, Mid1 expression is observed in the proliferative compartments of both dorsal midbrain and in the cerebellum anlage (Fig.10). By E13.5-E14.5 strong and specific expression in the tectum with a sharp caudal limit at the dorsal midbrain/hindbrain boundary (MHB) is observed (Dal Zotto et al., 1998). We analyzed markers expressed at the dorsal MHB at these stages (Wang and Zoghbi, 2001). We found no overt differences in the expression of several markers (e.g. Gbx2, Math1, En1, En2, Gli3) although they all suggested a mis-positioning of the boundary (Fig. 11).

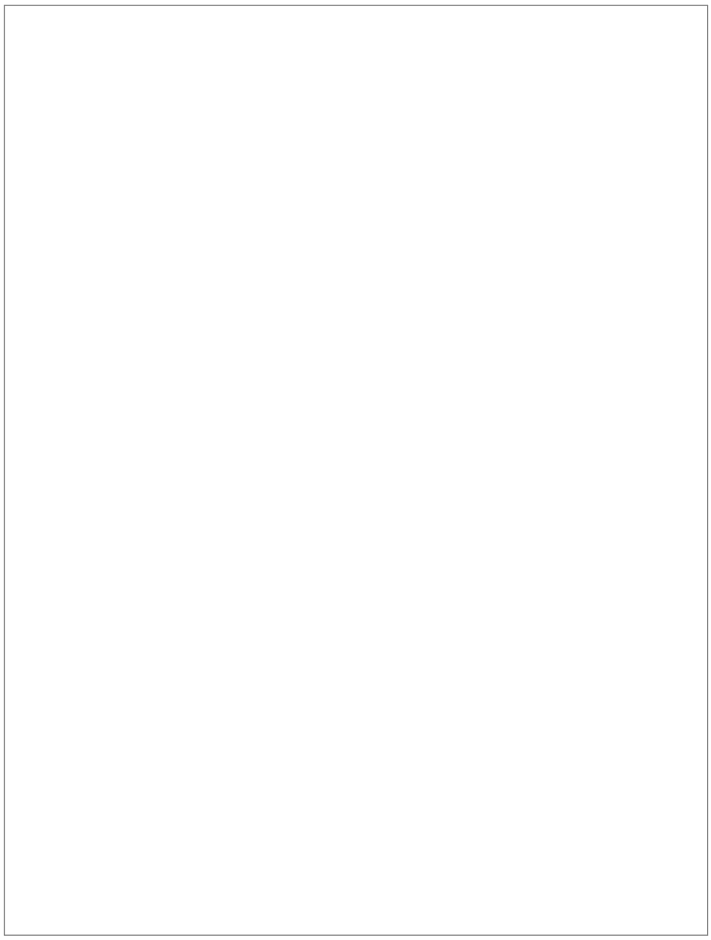

Fig. 10 - Expression of Mid1 in the dorsal midbrain and cerebellar region at E11.5, E12.5, and E13.5 as indicated; the line indicates the border between the dorsal midbrain (m) and hindbrain (h)

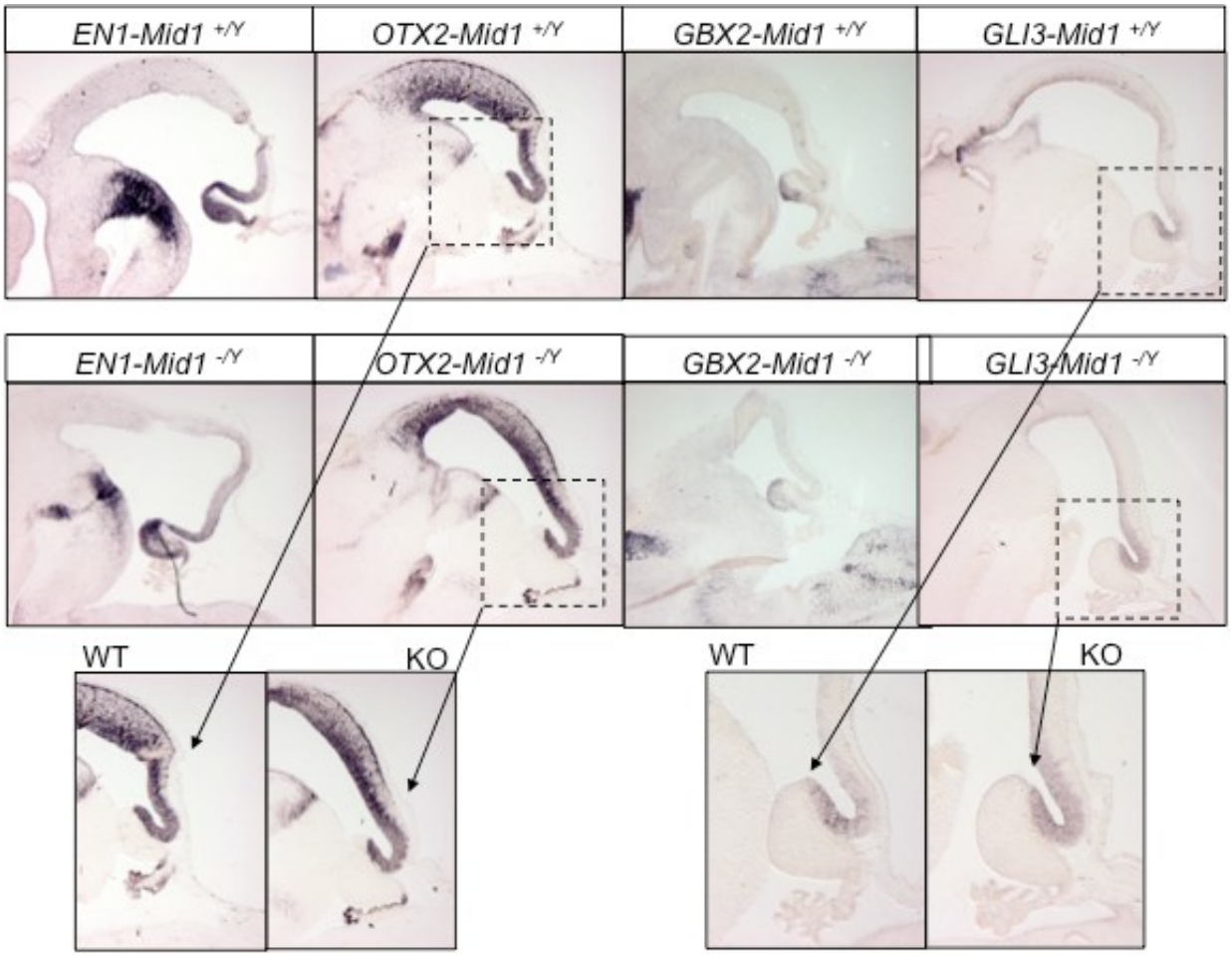

Fig.11 - In-situ Hybridisation of Otx2, Gbx2, En1 and Gli3 in WT and Mid1 null mice.
No differences are detected in the expression level, although they suggested a mis-positioning of the boundary (E=14.5).

This observation was further confirmed by the expression patterns of Pax2 (at this stage limited to the cerebellum) and Otx2 (expressed in the dorsal midbrain) that show a more rostral position

of the midbrain/cerebellum boundary in Mid1$^{-/Y}$ embryos resulting in a shorter lower portion of the IC (Fig. 12a-b). We measured the length of the IC, i.e. the distance between the posterior Otx2 expression limit and the IC physical bending on the ventricular side (asterisk in Fig. 12b), in Mid1$^{-/Y}$ (n=4) and Mid1$^{+/Y}$ (n=4) E14.5 embryos at three medio-lateral positions of the presumptive vermal region. As shown in the graph, the null mice have a shorter IC with the difference more pronounced in the lateral sections of the vermis (Fig. 12c).

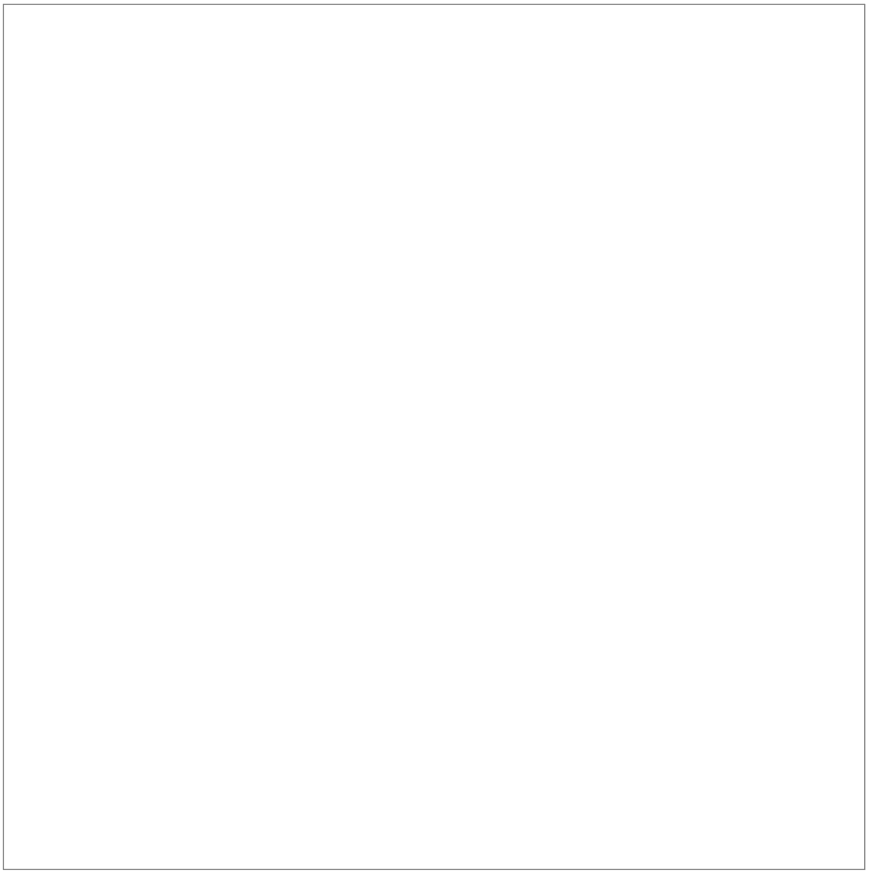

Fig.12 - Reduced IC length and rostralization of midbrain/cerebellar boundary in Mid1$^{-/Y}$ embryos. Overlay of images of adjacent E14.5 sagittal sections hybridized with Pax2 (green) and Otx2 (purple) (A, B). The arrow indicates the mis-positioning of the isthmus (B). (C) E14.5 IC length (mm) in wild-type (n=4) and null (n=4) mice. The length is the ventricular side distance between the two physical bending, indicated with the arrow and the asterisk in B, at three different positions of the vermal region: M, medial; M/L, medio-lateral (about 120 µm from the midline); L, lateral (about 240 µm from the midline). T test, **P =0.0042.

Although there is a trend towards a shorter IC, we do not observe statistically significant differences at E13.5. We tested programmed cell death occurrence in the IC at E12.5 - E14.5. Few cells are undergoing apoptosis in this region at these stages and they are not increased in null embryos. Similarly, we did not find overt differences in the proliferation of the IC using the anti-Ki67 antibody. Whatever the mechanism, the net effect of a shorter IC is a more anterior position of the dorsal midbrain/hindbrain boundary.

4.4 Fgf17 down-regulation in Mid1$^{-/Y}$ midbrain-hindbrain boundary

Fibroblast growth factors (Fgfs) are key molecules in the establishment and development of the dorsal midbrain-cerbellum border. Early in development Fgf8 is the main player in the isthmic organizer (IO), the signaling center that coordinates the patterning of the cerebellum at the mesencephalon/rhombomere 1 (mes/r1) boundary (Liu et al., 1999; Martinez et al., 1999). At mid-gestation, Fgf8 is involved in the proper A-P development of the mes/r1 region (Partanen, 2007). We analyzed Fgf8 at E10.5 and E12.5 and did not find alteration of its expression in null mice. Another member of the Fgf8 subfamily, Fgf17, is expressed at the mes/r1 boundary but, differently from Fgf8, its expression extends temporally and from E13.5 to E14.5 Fgf17 is the only Fgf expressed in this region (Xu et al., 2000). At E12.5 we did not observe changes in the expression of Fgf17. However, at E13.5 we began to observe a decrease in the Fgf17 expression

domain in Mid1$^{-/Y}$ mice in both medial and medio- lateral sagittal sections (Fig. 13a-d). The down-regulation of Fgf17 is striking at E14.5. At this stage in the mutant embryos, Fgf17 expression domain is maintained at the border between the IC and the cerebellar plate but heavily restricted along the antero-posterior axis (Fig. 13e-h). Analysis of coronal sections at the same stage confirmed the strong reduction of Fgf17 signal (Fig. 13i-l).

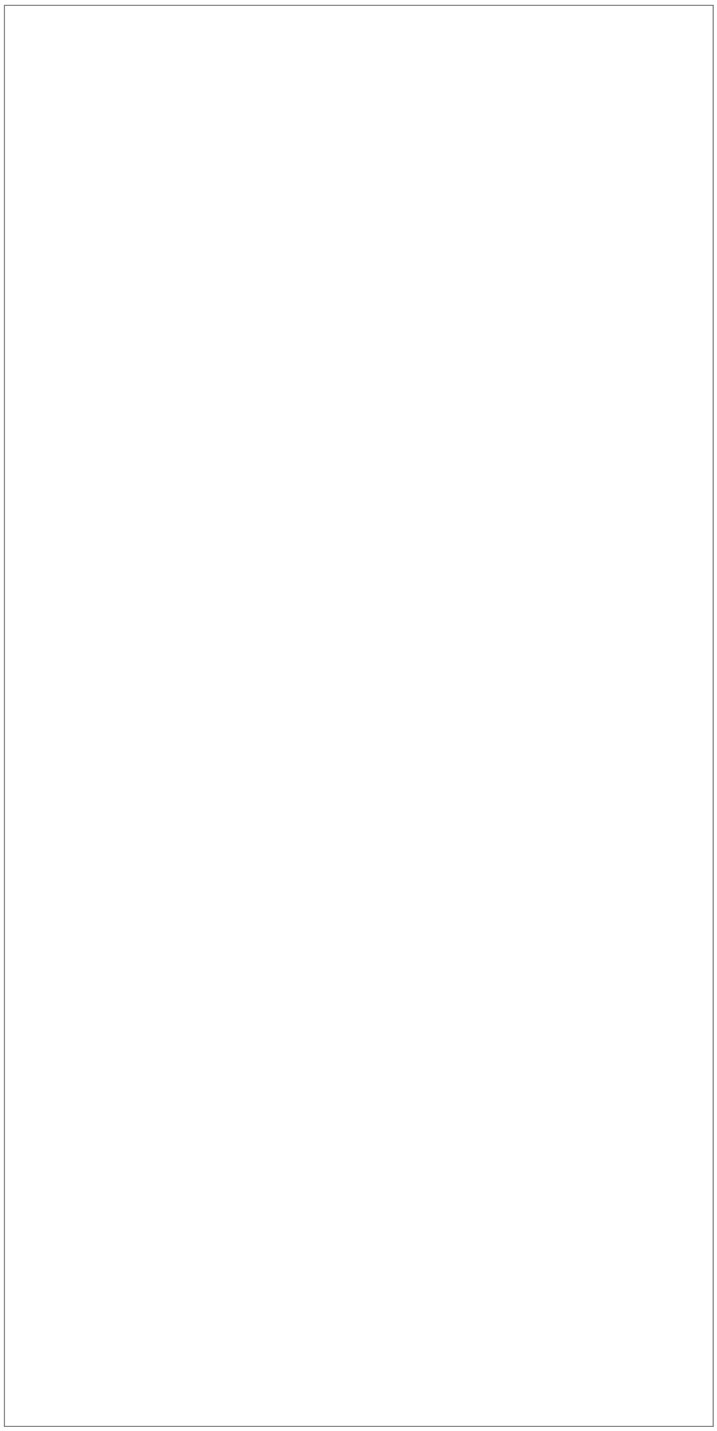

Fig.13 - Fgf17 is down-regulated in Mid1$^{-/Y}$ embryos. RNA in situ hybridization of Fgf17 on E13.5 sagittal section at (A, B, medial; C, D, medio-lateral); on E14.5 sagittal sections (E, F, medial; G, H, medio-lateral); and on E14.5 coronal sections (I, J, rostral; K, L, caudal). Down-regulation of Fgf17 in Mid1$^{-/Y}$ embryos starts at E13.5 and is more evident at E14.5 especially in the next to the midline region

along the medio-lateral axis and in the cerebellum along the antero-posterior axis. The line indicates the isthmus; m, midbrain; h, hindbrain.

Taken together, these data indicate that Mid1 is important for the determination of the boundary between the tectum and the cerebellum and for the expression of a key regulator of this region, Fgf17.

4.5 Mid1$^{-/Y}$ mice have motor coordination and motor learning impairment

Our collaborator investigated whether the abnormalities observed in Mid1$^{-/Y}$ mice correlates with cerebellum dependent behavioural functions. To test motor coordination, he used the walking and the hanging wire tasks (Joyal et al., 1996). He found that Mid1$^{-/Y}$ mice made more false steps walking on the inclined wire (wild-type: 5.5 ± 0.97 versus Mid1$^{-/Y}$: 9.077 ± 0.92; F1/26=7.181; p=0.01) and were also impaired in hanging on the wire compared to wild-type animals (latency to fall off the grid for wild-type: 61 ± 4.9 sec; for Mid1$^{-/Y}$: 42 ± 5.7 sec; F1/25=6.07; p=0.02). These effects were not due to muscular or primary sensorial deficits, since Mid1$^{-/Y}$ mice were not impaired in any of these tasks.

He tested motor learning in the classic rotarod task. Although both groups improved their performance across days, Mid1$^{-/Y}$ mice showed delayed motor learning (Fig. 14a). The observed impairment is not simply due to general hypo-activity since Mid1$^{-/Y}$ mice were hyperactive when compared to their wild-type littermates.

He also tested long-term habituation of the acoustic startle response, a form of non- associative learning selectively mediated by the cerebellar vermis and occurring when repeated exposure to an acoustic stimulus across days induces habituation of the startle response (Leaton and Supple, 1986). Whereas in the wild-type group the percentage of mean startle amplitude significantly

decreased from day 1 to day 3, no significant changes across days were observed in Mid1$^{-/Y}$ mice (Fig. 14b). Indeed, the percentage of startle response between the two groups significantly differed on the third day. Thus, Mid1$^{-/Y}$ vermal defect correlates with impairment in long-term habituation of acoustic startle.

The cerebellum has been also involved in other cognitive processes such as spatial learning, in particular in its egocentric form (Molinari et al., 1997; Petrosini et al., 1998). Our collaborator tested Mid1$^{-/Y}$ mice in the egocentric version of the cross maze task: food deprived animals are challenged to find food in a T-shaped maze in the absence of visual cues (Rinaldi et al., 2008). Mid1$^{-/Y}$ mice, as their wild-type littermates increased the percentage of correct responses across days (Fig. 14c). However, the percentage of correct responses in the two groups differs on the fourth and fifth training day, suggesting a delayed learning curve of Mid1$^{-/Y}$ animals. As control, he subjected different groups of animals to the allocentric version of the cross maze task, which has identical motor and motivational demand, but it is based on explicit learning and is dependent on the integrity of medial temporal lobe regions (Burguiere et al., 2005). Allocentric spatial learning requires the animal to form a cognitive map of the environment and learn the position of the food relatively to visual cues. The performance of Mid1$^{-/Y}$ mice in this non-procedural version of the cross-maze task was undistinguishable from wild-type animals (Fig. 14d).

Consistently, Mid1$^{-/Y}$ mice were not impaired in a medial temporal lobe dependent learning task, the passive avoidance. These results clearly prove that learning impairment of Mid1$^{-/Y}$ mice is not secondary to aspecific motor, sensorial, learning, memory or motivational impairments and well correlate with a vermal defect.

Together, these results demonstrate that Mid1 is important for the specification of the most anterior medial part of the cerebellum and that, compatibly with a cerebellar defect, its deletion

specifically affects motor coordination and non-associative and procedural lea

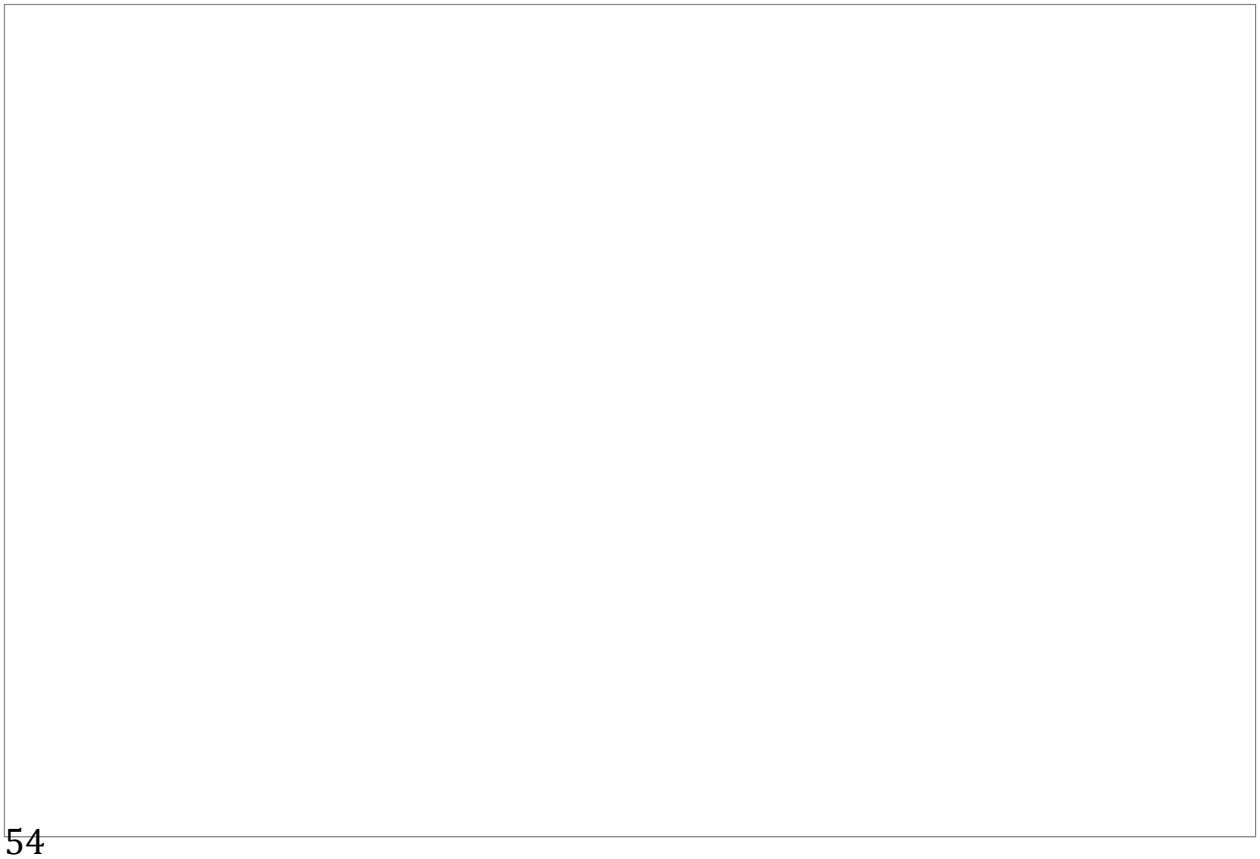

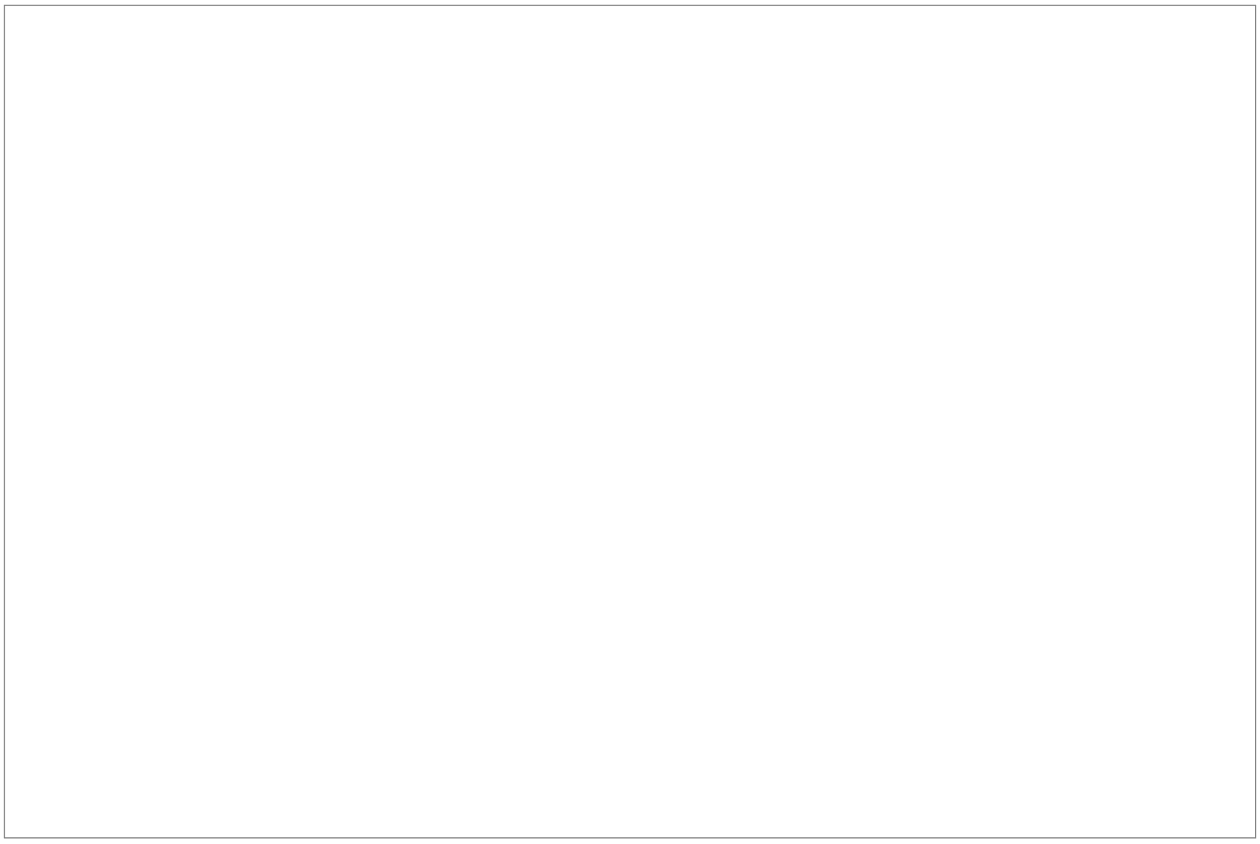

Fig.14 - Mid1 mice show motor coordination and learning impairments. (A) Mid1mice demonstrate a worse performance in the rotarod task, showing a deficit in motor learning acquisition ($F1/48=5.042$; $p=0.02$); (B) Control mice ($p=0.008$), but not $Mid1^{-/Y}$ mice, reduce the percentage of startle amplitude across days in the long-term habituation of acoustic startle task; the null mice do not habituate to the stimulus; the startle response between the two groups significantly differ on the third day ($p=0.02$); (C-D) $Mid1^{-/Y}$ mice recorded fewer correct responses in the egocentric spatial version of the cross-maze task (E) on the fourth ($p=0.01$) and on the fifth day ($p=0.06$), but not in the allocentric one (F).
*$p< 0.05$ $Mid1^{-/Y}$ versus wild-type.

4.6 Mid1$^{-/Y}$ null mice do not show any anatomical defects in other organs

In Opitz Syndrome patients not only cerebellar hypoplasia but also defects in other systems situated along the midline can be present. We have therefore investigated with hematoxilin-eosin staining and Masson's trichrome staining also the developing heart, palate, oesophagus and the urogenital tract that are often affected in this disorder. We have analysed the animals at different stages and in particular at E14.5, E16.5, E17.5, P0, P2 and adulthood. We did not find any differences between the control mice and the Mid1 null mice. In particular we stained paraffin sections of developing heart of WT and MID1 null mice with Masson Trichrome, but we did not find the presence of fibrosis or necrosis in the heart muscle and a normal morphology of the vases was present. Also the palate, esofagus and the urogenital tract were analyzed and the structures and the ducts were normal in size and morphology (Fig. 15)

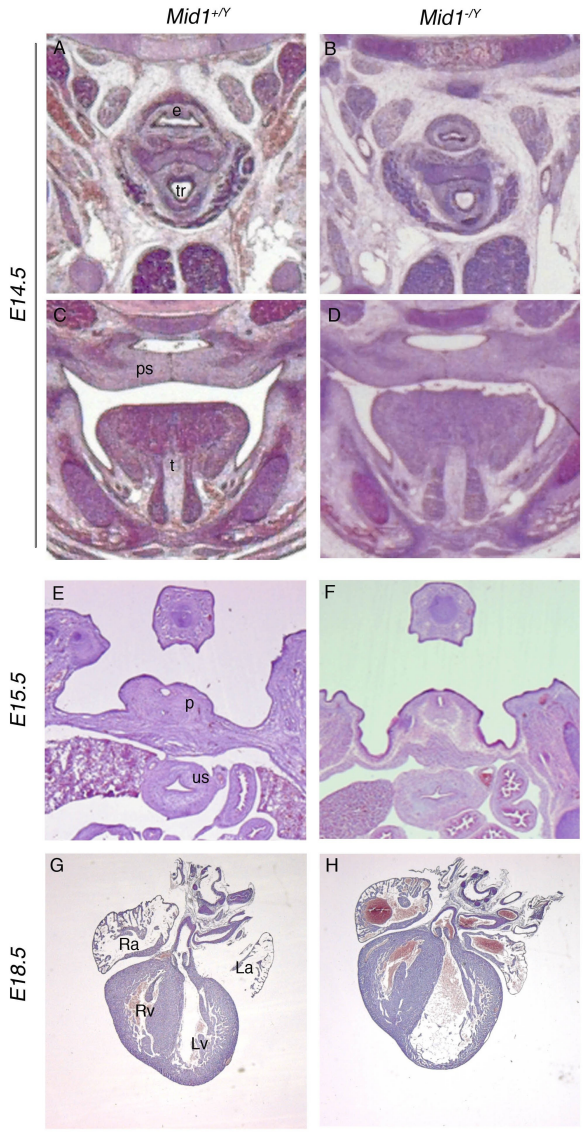

Fig. 15 - Normal development of non-neural midline structures in Mid1$^{-/Y}$ mice.
Representative images of H&E stained coronal E14.5 (A-D), transversal E15.5 (E and F), and frontal E18.5 (G and H) sections showing no detectable defects at the level of esophagous and trachea (A and B); in palatal closure (C and D); in the phallic part of the urethra and the urogenital sinus (future bladder) (E and F) and in the heart, where no major ventricular and atrial septal defects, the most frequent OS cardiac abnormalities, are detected (G and H). e, esophagous; tr, trachea; ps, palatal shelf; t, tongue; p, phallic part of urethra; us, urogenital sinus; Ra, right atrium; La, left atrium; Rv, right ventriculum; Lv, left ventriculum.

6. DISCUSSION

Here, we report the generation and characterization of a mouse line null for Mid1, the ortholog of the X-linked Opitz Syndrome gene, MID1. Like in human, the murine gene is transcribed from the X-chromosome and the hemizygous $Mid1^{-/Y}$ mice show a developmental phenotype, i.e. hypoplasia of the anterior region of the medial portion of the cerebellum, the vermis.

This mouse model perfectly recapitulates the anatomical central nervous system (CNS) defect observed in OS male patients with MID1 mutations, i.e. cerebellar vermis hypoplasia (Fontanella et al., 2008). Like many other clinical manifestations of OS, brain anatomical defects show variable expressivity and are not present in all patients. Indeed, there are cohorts with mild clinical presentations and in which brain defects were not observed (So et al., 2005). However, we recently reviewed the reports of OS patients with assessed MID1 mutations and found that more than one third of the patients subjected to MRI examination exhibit brain abnormalities. Moreover, the common brain defect in OS patients with MID1 mutations is hypoplasia of the cerebellar vermis (Cox et al., 2000; De Falco et al., 2003; Pinson et al., 2004; Fontanella et al., 2008). As part of the neurological involvement, OS patients often also present intellectual impairment and psychomotor and speech delays. We found that lack of the murine Mid1 gene results in motor coordination defects as well as motor, non-associative, and procedural learning impairments that may correlate with the developmental delays of OS patients. The cerebellum, traditionally associated with pure motor coordination functions, in the last decades has been linked more and more to cognitive responses (Molinari et al., 1997; Petrosini et al., 1998; Tavano et al., 2007). These studies mainly rely on individuals with

specific cerebellar lesions either as consequence of tumour surgery in human or experimentally induced in animal models. Consistent with behavioural data obtained upon selective lesion of the vermis, Mid1$^{-/Y}$ mice show hyperactivity, balance and motor coordination defects, motor and procedural learning deficits and lack of long-term habituation to acoustic startle (Leaton and Supple, 1986; Joyal et al., 1996; Molinari et al., 1997; Bobee et al., 2000; Callu et al., 2007). In the case of spatial egocentric learning, a major involvement of the hemispheres has been reported (Gaytan-Tocaven and Olvera-Cortes, 2004), however, our data suggest that the vermis may also contribute to this task. Together, behavioural deficits in Mid1$^{-/Y}$ mice qualitatively recapitulate those observed after selective lesions of the cerebellar vermis. Few animal models with specific defects in the anterobasal vermis are reported and much still needs to be unravelled of the function and connectivity of this portion of the cerebellum. This animal model will be useful to further dissect the function of the different domains of the vermis. As mentioned, in addition to the CNS defect OS patients show craniofacial, tracheo-esophageal, cardiac and urogenital midline abnormalities that are not present in Mid1 knock- out mice. In fact, the Mid1$^{-/Y}$ mice have a normal life span, they are fertile and born at the expected Mendelian ratio indicating that life-threatening defects such as laryngo-tracheo-esophageal (LTE) abnormalities, cleft palate, and major cardiac defects are not present in this mouse model. Moreover, histological analyses during prenatal development confirmed that: a) the LTE region and the palate develop normally; b) no signs of hypospadias are observed, being the urethra well canalized in the phallic portion in E15.5 embryos; and c) the major cardiac abnormalities presented by OS patients (ventricular and atrial septal defects) are not observed in E18.5 mice. Although we cannot exclude that subtle defects of midline structures might be present in the Mid1$^{-/Y}$ mice it is a fact that manifest abnormalities, other than the cerebellar defect, are not

present. The discrepancy between the human and the murine phenotype might be explained by the influence of the genetic background or by evolutionary developmental differences between the two species that may translate in different expressivity of the clinical signs. Indeed, Mid1 loss of function results in complete penetrance of developmental defects in both species while the expressivity of the midline defects is different, i.e. all the $Mid1^{-/Y}$ mice show the cerebellar defect and all OS patients with MID1 mutations show several midline signs, among which the cerebellar defect, with variable expressivity. The presence of a partially redundant gene that in the mouse is able to compensate the absence of Mid1 in non-neural compartments may underlie these differences. Natural candidate for this role is the close homolog of Mid1, Mid2 (Buchner et al., 1999). Mid2 belongs to the same family and interacts with Mid1 (Short et al., 2002). Functional redundancy between Mid1 and Mid2 has been demonstrated in chick. In fact, the effect of the down-regulation of a cascade of genes in the Hensen's node in chick embryos exerted by an anti-Mid1/2 morpholino can be rescued by the expression of either of the two genes (Granata et al., 2005). The expression of Mid2 in $Mid1^{-/Y}$ embryos observed by both RNA in situ hybridization and real time PCR is not altered (data not shown) but redundancy may act through different mechanisms. Mid1/2 functional cooperation is an interesting issue to address also in the perspective of better understanding the high variability of the clinical manifestations in OS patients even carrying the same MID1 mutation.

We demonstrated that lack of Mid1 causes the abnormal development of the lobes that derive from the anterobasal cardinal lobe, the most anterior part of the developing vermis adjacent to the tectum. Absence of Mid1 causes a shortening of the E14.5 IC lower region with a consequent rostralization of the dorsal isthmus, the region at the boundary between the

midbrain and hindbrain. This rostralization is concomitant with reduction in Fgf17 expression. As said, Fgf17 is a member of the subfamily of Fgfs expressed in the mes/rh1 boundary (Fgf8, 17, and 18) and is the only one expressed in this region from E13.5 to E14.5 when the other two have already been switched off (Xu et al., 1999; Xu et al., 2000).

Consistent with our data, the complete lack of Fgf17 leads to malformation of the anterior vermis caused by an anticipated rostral differentiation of PCs (Xu et al., 2000). Moreover, in Fgf17 null brains the inferior colliculus is highly hypoplastic (Xu et al., 2000). The IC phenotype in Mid1$^{-/Y}$ mice is milder than in the Fgf17 mutant. This is very likely due to the fact that we do not have complete loss of Fgf17 expression but a strong reduction limited to a short window of time. On the contrary, the cerebellar phenotype appears more severe in the Mid1$^{-/Y}$ than in the Fgf17$^{-/-}$ mice suggesting that Fgf signaling might not be the only mechanism implicated. However, we observed the presence of ectopic PCs in very rostral cerebellar/isthmic position consistent with the premature differentiation of PCs in the rostro-medial part of the cerebellar plate proposed for the Fgf17$^{-/-}$ mice. Although we still do not know if the reduction of Fgf17 is caused by a transcriptional mechanism or by the absence of the midbrain/hindbrain boundary cells deputed to express it, the regulation of a member of the Fgf family by Mid1 is not unprecedent. Indeed, data in chick embryos indicated a positive downstream effect of Mid1/2 on the expression of Fgf8 in the ectoderm of the Hensen's node (Granata and Quaderi, 2003).

What is the mechanism through which Mid1 absence causes shortening of the IC, down-regulation of Fgf17 and defects in the development of the anterobasal lobe is still to be determined. Major changes in proliferation and apoptosis do not seem to account for the reduction of the IC and rostralization of the isthmus, at least at E12.5 – 13.5 stages. The

cerebellum, the tectum and the isthmic region are also affected in other mouse knock-out lines among which are the series of Gli3 mutants (Blaess et al., 2008).

Interestingly, Gli3 is expressed, like Mid1, in the dorsal tectum at mid-gestation and GLI3 is implicated in three human pathological conditions sharing common features with Opitz Syndrome (Biesecker, 2006). A fascinating hypothesis is that Mid1 might modulate Gli3 activity in the midbrain/cerebellar region by controlling PP2A levels (Krauss et al., 2008). Through this or other mechanisms, Mid1 may influence the migration, adhesion, or identity of the population of dorsal midbrain/hindbrain boundary cells that are crucial for the maintenance of the proper lineage separation between the two structures (Broccoli et al., 1999; Kala et al., 2008).

This mouse model will be crucial to determine the pathogenetic mechanisms and the physiological function of Mid1 during development, mechanisms that can be studied exploiting the cerebellar defect as a system but that can be relevant also in the occurrence of the other clinical manifestations of OS as well as in other human congenital disorders presenting the same signs.

7. REFERENCES

Adams KA, Maida JM, Golden JA, Riddle RD (2000) The transcription factor Lmx1b maintains Wnt1 expression within the isthmic organizer. Development 127(9): 1857-67.

Alder J, Lee KJ, Jessell TM, Hatten ME (1999) Generation of cerebellar granule neurons in vivo by transplantation of BMP-treated neural progenitor cells. Nat Neurosci 2(6): 535-40.

Ang SL, Jin O, Rhinn M, Daigle N, Stevenson L, Rossant J (1996) A targeted mouse Otx2 mutation leads to severe defects in gastrulation and formation of axial mesoderm and to deletion of rostral brain. Development 122 (1): 243-52.

Biesecker LG (2006) What you can learn from one gene: GLI3. J Med Genet 43:465-469.

Blaess S, Stephen D, Joyner AL (2008) Gli3 coordinates three-dimensional patterning and growth of the tectum and cerebellum by integrating Shh and Fgf8 signaling. Development135: 2093-2103.

Bobee S, Mariette E, Tremblay-Leveau H, Caston J (2000) Effects of early midline cerebellar lesion on cognitive and emotional functions in the rat. Behav Brain Res 112: 107-117.

Broccoli V, Boncinelli E, Wurst W (1999) The caudal limit of Otx2 expression positions the isthmic organizer. Nature 401:164-168.

Buchner G, Montini E, Andolfi G, Quaderi N, Cainarca S, Messali S, Bassi MT, Ballabio A, Meroni G, Franco B (1999) MID2, a homologue of the Opitz syndrome gene MID1: similarities

in subcellular localization and differences in expression during development. Hum Mol Genet 8:1397-1407.

Burguiere E, Arleo A, Hojjati M, Elgersma Y, De Zeeuw CI, Berthoz A, Rondi-Reig L (2005) Spatial navigation impairment in mice lacking cerebellar LTD: a motor adaptation deficit? Nat Neurosci 8:1292-1294.

Cainarca S, Messali S, Ballabio A, Meroni G (1999) Functional characterization of the Opitz syndrome gene product (midin): evidence for homodimerization and association with microtubules throughout the cell cycle. Hum Mol Genet 8:1387-1396.

Callu D, Puget S, Faure A, Guegan M, El Massioui N (2007) Habit learning dissociation in rats with lesions to the vermis and the interpositus of the cerebellum. Neurobiol Dis 27:228-237.

Chizhikov V, Millen KJ (2003) Development and malformations of the cerebellum in mice. Mol Genet Metab 80: 54-65.

Cox TC, Allen LR, Cox LL, Hopwood B, Goodwin B, Haan E, Suthers GK (2000) New mutations in MID1 provide support for loss of function as the cause of X-linked Opitz syndrome. Hum Mol Genet 9:2553-2562.

Dal Zotto L, Quaderi NA, Elliott R, Lingerfelter PA, Carrel L, Valsecchi V, Montini E, Yen CH, Chapman V, Kalcheva I, Arrigo G, Zuffardi O, Thomas S, Willard HF,

Ballabio A, Disteche CM, Rugarli EI (1998) The mouse Mid1 gene: implications for the pathogenesis of Opitz syndrome and the evolution of the mammalian pseudoautosomal region. Hum Mol Genet 7:489-499.

De Falco F, Cainarca S, Andolfi G, Ferrentino R, Berti C, Rodriguez Criado G, Rittinger O, Dennis N, Odent S, Rastogi A, Liebelt J, Chitayat D, Winter R, Jawanda H,

Ballabio A, Franco B, Meroni G (2003) X-linked Opitz syndrome: novel mutations in the MID1 gene and redefinition of the clinical spectrum. Am J Med Genet 120A:222- 228.

Favor J, Sandulache R, Neuhäuser-Klaus A, Pretsch W, Chatterjee B, Senft E, Wurst W, Blanquet V, Grimes P, Spörle R, Schughart K (1996) The mouse Pax2(1Neu) mutation is identical to a human PAX2 mutation in a family with renal-coloboma syndrome and results in developmental defects of the brain, ear, eye, and kidney. Proc Natl Acad Sci USA 93(24):13870-5.

Fontanella B, Russolillo G, Meroni G (2008) MID1 mutations in patients with X-linked Opitz G/BBB syndrome. Hum Mutat 29:584-594.

Gaytan-Tocaven L, Olvera-Cortes ME (2004) Bilateral lesion of the cerebellar-dentate nucleus impairs egocentric sequential learning but not egocentric navigation in the rat. Neurobiol Learn Mem 82:120-127.

Gaudenz K, Roessler E, Quaderi N, Franco B, Feldman G, Gasser DL, Wittwer B, Horst J, Montini E, Opitz JM, Ballabio A, Muenke M. Opitz G/BBB syndrome in Xp22: mutations in the MID1 gene cluster in the carboxy-terminal domain. Am J Hum Genet. 1998; 63: 703–10.

Granata A, Quaderi NA (2003) The Opitz syndrome gene MID1 is essential for establishing asymmetric gene expression in Hensen's node. Dev Biol 258:397-405.

Granata A, Savery D, Hazan J, Cheung BM, Lumsden A, Quaderi NA (2005) Evidence of functional redundancy between MID proteins: implications for the presentation of Opitz syndrome. Dev Biol 277:417-424.

Joyal CC, Meyer C, Jacquart G, Mahler P, Caston J, Lalonde R (1996) Effects of midline and lateral cerebellar lesions on motor coordination and spatial orientation. Brain Res 739:1-11.

Kala K, Jukkola T, Pata I, Partanen J (2008) Analysis of the midbrain-hindbrain boundary cell fate using a boundary cell-specific Cre-mouse strain. Genesis 46: 29-36.

Krauss S, Foerster J, Schneider R, Schweiger S (2008) Protein phosphatase 2A and rapamycin regulate the nuclear localization and activity of the transcription factor GLI3. Cancer Res 68:4658-4665.

Leaton RN, Supple WF, Jr. (1986) Cerebellar vermis: essential for long-term habituation of the acoustic startle response. Science 232: 513-515.

Llinas RR, Walton KD, Lang EJ (2004). The Synaptic Organization of the Brain. Oxford University ISBN 0195159551.

Liu A, Losos K, Joyner AL (1999) FGF8 can activate Gbx2 and transform regions of the rostral mouse brain into a hindbrain fate. Development 126: 4827-4838.

Liu J, Prickett TD, Elliott E, Meroni G, Brautigan DL (2001) Phosphorylation and microtubule association of the Opitz syndrome protein mid-1 is regulated by protein phosphatase 2A via binding to the regulatory subunit alpha 4. Proc Natl Acad Sci U S A 98:6650-6655.

Martinez S, Crossley PH, Cobos I, Rubenstein JL, Martin GR (1999) FGF8 induces formation of an ectopic isthmic organizer and isthmocerebellar development via a repressive effect on Otx2 expression. Development 126: 1189-1200.

McMahon AP, Joyner AL, Bradley A, McMahon JA (1992) The midbrain-hindbrain phenotype of Wnt-1-/Wnt-1- mice results from stepwise deletion of engrailed-expressing cells by 9.5 days postcoitum. Cell 69(4): 581-95.

Meroni G, Diez-Roux G (2005) TRIM/RBCC, a novel class of 'single protein RING finger' E3 ubiquitin ligases. Bioessays 27:1147-1157.

Meyers EN, Lewandoski M, Martin GR (1998) An Fgf8 mutant allelic series generated by Cre- and Flp-mediated recombination. Nat Genet 18(2): 136-41.

Millet S, Campbell K, Epstein DJ, Losos K, Harris E, Joyner AL (1999) A role for Gbx2 in repression of Otx2 and positioning the mid/hindbrain organizer. Nature 401(6749):161-4.

Mnayer L, Khuri S, Merheby HA, Meroni G, Elsas LJ. A structure-function study of MID1 mutations associated with a mild Opitz phenotype. Mol Genet Metab. 2006; 87: 198–203.

Molinari M, Grammaldo LG, Petrosini L (1997a) Cerebellar contribution to spatial event processing: right/left discrimination abilities in rats. Eur J Neurosci 9:1986-1992.

Molinari M, Leggio MG, Solida A, Ciorra R, Misciagna S, Silveri MC, Petrosini L (1997b) Cerebellum and procedural learning: evidence from focal cerebellar lesions. Brain 120 (Pt 10):1753-1762.

Opitz JM, Frias JL, Gutenberger JE, Pellet JR. The G syndrome of multiple congenital anomalies. Birth defects: Original Article Series (V)2: 95-102. 1969

Opitz JM, Summitt RL, Smith DW. The BBB syndrome familial telecanthus with associated congenital anomalies. Birth Defects: Original Article Series (V)2: 86-94. 1969

Opitz JM (1987) G syndrome (hypertelorism with esophageal abnormality and hypospadias, or hypospadias-dysphagia, or "Opitz-Frias" or "Opitz-G" syndrome)-- perspective in 1987 and bibliography. Am J Med Genet 28: 275-285.

Palmer S, Perry J, Kipling D, Ashworth A (1997) A gene spans the pseudoautosomal boundary in mice. Proc Natl Acad Sci U S A 94:12030-12035.

Partanen J (2007) FGF signalling pathways in development of the midbrain and anterior hindbrain. J Neurochem 101:1185-1193.

Petrosini L, Leggio MG, Molinari M (1998) The cerebellum in the spatial problem solving: a co-star or a guest star? Prog Neurobiol 56:191-210.

Pinson L, Auge J, Audollent S, Mattei G, Etchevers H, Gigarel N, Razavi F, Lacombe D, Odent S, Le Merrer M, Amiel J, Munnich A, Meroni G, Lyonnet S, Vekemans M, Attie-Bitach T (2004) Embryonic expression of the human MID1 gene and its mutations in Opitz syndrome. J Med Genet 41:381-386.

Prickett TD, Brautigan DL (2007) Cytokine activation of p38 mitogen-activated protein kinase and apoptosis is opposed by alpha-4 targeting of protein phosphatase 2A for site-specific dephosphorylation of MEK3. Mol Cell Biol 27:4217-4227.

Quaderi NA, Schweiger S, Gaudenz K, Franco B, Rugarli EI, Berger W, Feldman GJ, Volta M, Andolfi G, Gilgenkrantz S, Marion RW, Hennekam RCM, Opitz JM, Muenke M, Ropers HH, Ballabio A (1997) Opitz G/BBB syndrome, a defect of midline development, is due to mutations in a new RING finger gene on Xp22. Nature Genetics 17:285-291.

Reifers F, Böhli H, Walsh EC, Crossley PH, Stainier DY, Brand M (1998) Fgf8 is mutated in zebrafish acerebellar (ace) mutants and is required for maintenance of midbrain-hindbrain boundary development and somitogenesis. Development 125(13): 2381-95.

Richman JM, Fu KK, Cox LL, Sibbons JP, Cox TC (2002) Isolation and characterisation of the chick orthologue of the Opitz syndrome gene, Mid1, supports a conserved role in vertebrate development. Int J Dev Biol 46:441-448.

Rinaldi A, De leonibus E, Cifra A, Minicocci E, Oliverio A, Mele A (2008) Neural network activated during allocentric and egocentric spatial memory retrieval in mice: focus on striatal subregions. FENS Abstr 4:157.124.

Robin NH, Opitz JM, Muenke M (1996) Opitz G/BBB syndrome: clinical comparisons of families linked to Xp22 and 22q, and a review of the literature. Am J Med Genet 62:305-317.

Robin NH, Feldman GJ, Aronson AL, Mitchell HF, Weksberg R, Leonard CO, Burton BK, Josephson KD, Laxova R, Aleck KA, Allanson JE, Guion-Almeida ML, Martin RA, Leichtman LG, Price RA, Opitz JM, Muenke M (1995) Opitz syndrome is genetically heterogeneous, with one locus on Xp22, and a second locus on 22q11.2. Nat Genet 11:459-461.

Schweiger S, Foerster J, Lehmann T, Suckow V, Muller YA, Walter G, Davies T, Porter H, van Bokhoven H, Lunt PW, Traub P, Ropers HH (1999) The Opitz syndrome gene product, MID1, associates with microtubules. Proc Natl Acad Sci U S A 96:2794- 2799.

Shaw A, Longman C, Irving M, Splitt M. Neonatal teeth in X-linked Opitz (G/BBB) syndrome. Clin Dysmorphol. 2006; 15: 185–6.

Short KM, Hopwood B, Yi Z, Cox TC (2002) MID1 and MID2 homo- and heterodimerise to tether the rapamycin- sensitive PP2A regulatory subunit, Alpha 4, to microtubules: implications for the clinical variability of X-linked Opitz GBBB syndrome and other developmental disorders. BMC Cell Biol 3:1.

Sillitoe RV, Joyner AL (2007) Morphology, molecular codes, and circuitry produce the three-dimensional complexity of the cerebellum. Annu Rev Cell Dev Biol 23:549-577. So J et al. (2005) Mild phenotypes in a series of patients with Opitz GBBB syndrome with MID1 mutations. Am J Med Genet A 132:1-7.

Surace EM, Angeletti B, Ballabio A, Marigo V (2000) Expression pattern of the ocular albinism type 1 (Oa1) gene in the murine retinal pigment epithelium. Invest Ophthalmol Vis Sci 41:4333-4337.

Tavano A, Grasso R, Gagliardi C, Triulzi F, Bresolin N, Fabbro F, Borgatti R (2007) Disorders of cognitive and affective development in cerebellar malformations. Brain 130:2646-2660.

Trockenbacher A, Suckow V, Foerster J, Winter J, Krauss S, Ropers HH, Schneider R, Schweiger S (2001) MID1, mutated in Opitz syndrome, encodes an ubiquitin ligase that targets phosphatase 2A for degradation. Nat Genet 29:287-294.

Urbánek P, Fetka I, Meisler MH, Busslinger M. (1997) Cooperation of Pax2 and Pax5 in midbrain and cerebellum development. Proc Natl Acad Sci USA 94(11): 5703-8.

Wang VY, Zoghbi HY (2001) Genetic regulation of cerebellar development. Nat Rev Neurosci 2:484-491.

Wassarman KM, Lewandoski M, Campbell K, Joyner AL, Rubenstein JL, Martinez S, Martin GR (1997) Specification of the anterior hindbrain and establishment of a normal mid/hindbrain organizer is dependent on Gbx2 gene function. Development 124(15): 2923-24

Winter J, Lehmann T, Suckow V, Kijas Z, Kulozik A, Kalscheuer V, Hamel B, Devriendt K, Opitz J, Lenzner S, Ropers HH, Schweiger S (2003). Duplication of the MID1 first exon in a patient with Opitz G/BBB syndrome. Hum Genet. 112: 249–54.

Xu J, Liu Z, Ornitz DM (2000) Temporal and spatial gradients of Fgf8 and Fgf17 regulate proliferation and differentiation of midline cerebellar structures. Development 127: 1833-1843.

Xu J, Lawshe A, MacArthur CA, Ornitz DM (1999) Genomic structure, mapping, activity and expression of fibroblast growth factor 17. Mech Dev 83:165-178.

Zhang XM, Lin E, Yang XJ (2000) Sonic hedgehog-mediated ventralization disrupts formation of the midbrain-hindbrain junction in the chick embryo. Dev Neurosci 22(3): 207-16.